Institute of Mechanical Engineering
and Energy Technology

Lucerne University of
Applied Sciences and Arts

HOCHSCHULE
LUZERN

MSE - Specialization project 1

Cooling concept for Hyperloop pod prototypes

Author: Manuel Häusler

Advisors: Prof. Dr. Ulf Christian Müller
Thomas Sergi

Experts: Dr. Peter Neuschwander

Industrial partner: Swissloop
Leonhardstrasse 27
CH-8092 Zürich

Horw, 21 June 2019

Declaration of Authorship

I hereby declare that I have prepared the present work independently and have used nothing other than the specified aids. All text sections, citations or contents of other authors used have been explicitly marked as such.

Horw, 21 June 2019

Manuel Häusler

Ich bin der Author

Digital signiert von Manuel Häusler

Datum: 2019.09.18 08:27:42 +0200

Abstract

The Hyperloop concept is a theoretical concept for a new mode of transport that levitates in partial vacuum tubes at almost the speed of sound. The interest in this technology and its advantages for the society is constantly growing. This trend can be seen worldwide and rated in the amount of arising researches and prototypes.

Until now no solution is available how to cool the heat generating components of a Hyperloop vehicle. In this thesis a high-level design of a possible cooling concept for a Hyperloop vehicle is developed. To quantify the thermal losses a numerical model of the system is created. For that the Hyperloop Pod 2019 from Swissloop is used as the reference system. Findings from this model help to evaluate the cooling system and to optimise the load profile for the Swissloop Pod participating in the SpaceX Hyperloop Competition 2019.

The proposed cooling concept is based on a latent thermal storage. It is charged by the waste heat of the vehicle during the run in the vacuum tube. The calcium chloride hexahydrate is a PCM with the required capacity and performance characteristics. The PCMs melting point of 30°C makes it possible to regenerate the storage during the stops at the stations with cold tap water. The major heat source of a LIM powered Hyperloop pod is the winding of the motor which must be protected from overheating by internal cooling in the copper wires. The battery cells and the inverter are other relevant heat sources. The battery cells are directly flowed around by the cooling fluid and the inverter modules are cooled with a water cooler block and an in-line, controlled Peltier element.

Contents

Nomenclature

112S3P	3 lines in parallel with each 112 in series
EES	ElectricalEnergyStorage Library. Free modelica library that contains models with different complexity for simulating of electric energy storages like batteries (single cells as well as stacks).
IGBT	Insulated-gate bipolar transistor
LIM	Linear induction motor. An alternating current (AC), asynchronous linear motor that works by the same general principles as any other induction moto but with linear rotor and stator and thus linear thrust
LiPo	Lithium Polymer. A modern technology for galvanic cells
MSL	Modelica standard library. Free (standard conforming) library from the Modelica Association to model mechanical, electrical, magnetic, thermal, fluid, control systems and hierarchical state machines. Also numerical functions and functions for strings, files and streams are included.
OCV	Open circuit voltage. The electric potential provided by a electrical voltage source when disconnected from any circuit
PCM	Phase change material. A metrial which has its phase change region (solid-liquid) in the temperature range of the application temperature
SOC	State of charge. Number for the charging level of a cell
TES	Thermal energy storage.
HSR	High speed rails. Trains which operate completely or partly above 250 km/h by using the wheel-rail technology
Pod	The name of the vehicle used in a Hyperloop system. It is a small transportation unit which will drive independently through the Hyperloop tube network.

List of Figures

List of Tables

Chapter 1
Introduction

1.1 Project Background

Ever since, there was the wish of mankind for mobility. To travel around, or to transport goods with the least possible effort in the shortest possible time. This dream was always a fight against the ground friction, but also against the air drag of physics. In the early days the only way was to carry or pull along the goods by human or animal power. A first invention to minimize the effort was the sled, through which the contact area between the goods and the ground was reduced for the first time. The next great achievement was the wheel and later its progression to the wheel-rail combination. With that, friction was reduced to a minimum. Modern high speed trains (HSR) based on the wheel-rail technology are operating in speeds up to 350 km/h with comparatively low energy consumption. With the successful development and operation of levitation technology, the friction could be completely eliminated and only the air drag remains. As an example for such a system, the Japanese Chuo-Shinkansen will start its regular operation with speeds of 500 km/h between Tokio and Osaka in the near future. [1]

But what if we want to reach even higher speeds?

1.1.1 The Hyperloop concept

The first publication describing a Hyperloop concept can be found in «Berliner Illustrirte Zeitung» Nr. 33 from 1938.[2] There Hermann Kemper describes a transportation system which levitates inside an evacuated tube named «Rohrbahn». He thought about the technology as a kind of tube mail for people achieving incredible speeds. He is also considered to be the inventor of the magnetic levitation technology. In 1937 he patented the concept of magnetic levitation by controlled electromagnets where he mentioned the principle of his «Rohrbahn». [3] He wrote, that with airtight wagons in diluted air tubes, the driving resistance could be kept to a minimum even at highest speeds.

Figure 1.1: Hermann Kempers «Rohrbahn» from 1937 [2]

But at that time the technology was not ready to realize such a system. Nevertheless, the idea of the Hyperloop concept was born at that time.

The system described by Kemper fulfills the three main facets of the Hyperloop concept as it is understood today:

1. Vacuum or low-pressure environment for reducing drag. In an atmospheric pressure environment the air drag limits the maximum possible speed of a vehicle. By reducing the ambient pressure the air drag becomes very small even for highest speeds. Besler has been looking for an optimal ambient pressure to get the best compromise between remaining air drag and energy needed to maintain the pressure.[4]
2. Levitation or hovering. To get rid of friction, a contactless carrying and guiding system is needed. Possible technologies are magnetic levitation or hovering on an air cushion.
3. Efficient linear accelerator. A direct translation of the energy into a translatory motion without additional mechanics which will produce unnecessary friction. A propulsion with a linear accelerator is more efficient than a rotatory machine and its following transformation to a linear movement.

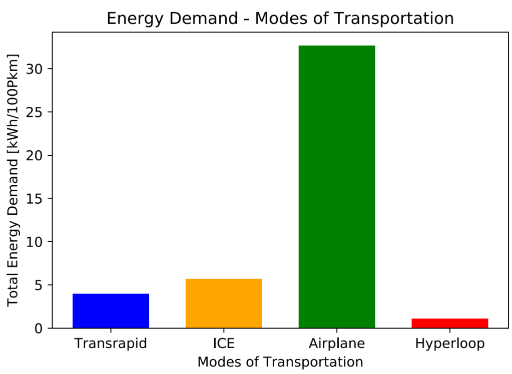

Figure 1.2: Comparison of energy demand for different modes of transport [4]

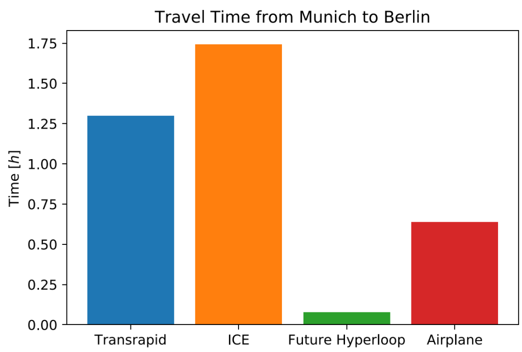

Figure 1.3: Comparison of travel time for different modes of transport [4]

With a system fulfilling the Hyperloop concept, enormous speeds can be realised on floor level. Besler compared different transportation systems on a hypothetical track between Munich and Berlin in terms of energy needed and traveling time.[4] In Fig.1.2 and Fig.1.3 one can see the results of his studies. In case an adequate pressure level is maintained inside the tubes, the Hyperloop outperforms the other modes of transport in both energy consumption and traveling time.

Another visulisation of that fact is the «von Kármán–Gabrielli» diagram. This diagram compares the efficiency of different modes of transportation by plotting the dimensionless number for resistance (called specific resistance) against velocity. The «von Kármán–Gabrielli» diagram in Fig. 1.4 compares the most important modes of transport by its qualitative placement. The red line is the so called «von Kármán–Gabrielli» limit line of vehicular performances which is a physical limit for all transportation modes at atmospheric pressure due to air drag. A more reliable «von Kármán–Gabrielli» can be found in «What price of speed»[5].

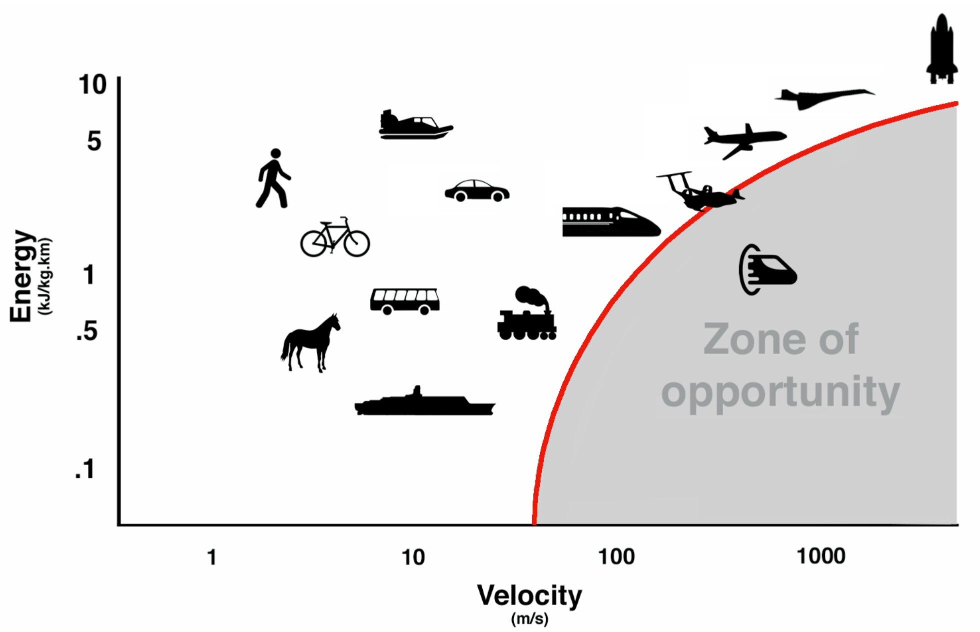

Figure 1.4: Qualitative comparison of different modes of transport using the «von Kármán–Gabrielli» diagram

After spending several years of thinking around the topic of Hyperloop systems, it can be expected that the Hyperloop will be the solution for long distance, intercontinental traveling. Arguments such as speed, energy efficiency, independence from fossil fuels or security will make their contribution to it.

1.1.2 Hyperloop Alpha

In 2013, Elon Musk wrote a paper named Hyperloop Alpha where he describes his idea of an innovative new technology for a high speed track between Los Angeles and San Francisco. In his version of the Hyperloop there are small trains (pods) for about 28 people accelerated by a linear induction motor (LIM) at the station exit. The levitation of the pod is realised by an air bearing suspension. For this purpose the air in front of the pod is collected, compressed and exhausted again in a kind of air bearing skids which provides the air cushion for the pod to hover. The partially evacuated steel tubes (one for each direction) are elevated on pillars and covered on the top by photovoltaic panels. The panels supply the system with the necessary energy and partially prevent the tubes for heating up in the sun.

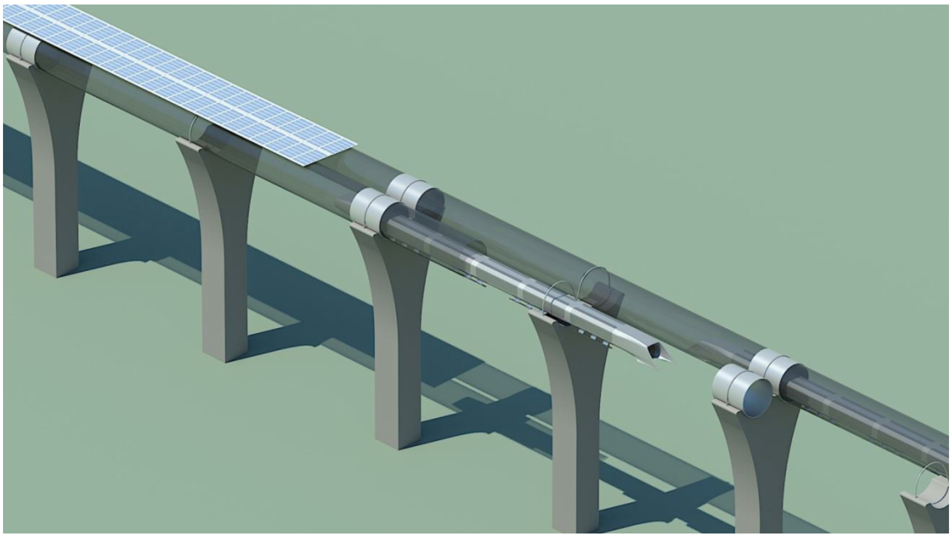

Figure 1.5: Visualisation of the Hyperloop Alpha [6]

In his paper, Musk discloses all his ideas, calculations and visualisations and in the end he passes everything further including the realisation back to his readers:

> Hyperloop is considered an open source transportation concept. The authors encourage all members of the community to contribute to the Hyperloop design process. Iteration of the design by various individuals and groups can help bring Hyperloop from an idea to a reality.[6]

With that paper Musk raised worldwide interest and many teams are now challenging themselves to successfully bring the technology of Hyperloop to reality.

Project website:

https://www.spacex.com/Hyperloopalpha

1.1.3 Swissloop

Swissloop was founded in 2016 by Swiss students as an independent association. The objective of Swissloop is to develop next-generation vehicles to participate and win the yearly Hyperloop pod competition realised by SpaceX in Los Angeles. In the long run the vision of Swissloop is the promotion and progression of Hyperloop technologies in Switzerland. As a platform, Swissloop connects students from various backgrounds to share resources and create a network to make the vision a reality.

The Hyperloop pods developed by Swissloop are designed to reach highest speed and in doing so fulfill the requirements of the competition. The innovations are accordingly limited by the existing infrastructure of SpaceX. Nevertheless, Swissloop was able to bring the Hyperloop concept to a wide audience in Switzerland and created a huge media interest for the Hyperloop technology.

Project website:

https://www.swissloop.ch

1.1.4 EuroTube

EuroTube is a very young non-profit research organisation with the aim to develop technologies and build testing infrastructures for vacuum transportation technologies in Europe. In collaboration with SBB and the Canton of Valais, EuroTube is planning and building the first research and test infrastructure for ultra-high-speed vacuum transportation on ground level with a 3km long test track in the Canton of Valais.[7]

Project website:

https://www.eurotube.org

1.2 Task definition

The present work is intended to analyse and quantify the heat sources on a representative Hyperloop pod for a defined load profile. A cooling concept should then be developed with the necessary power and capacity and meeting the following criteria:

- Low energy consumption
- Light and compact design
- Environmentally friendly materials and working fluids
- Connection of several heat sources and heat sinks
- Scalable to full-scale Hyperloop
- Economically

1.3 Procedure of the task

The first step is to quantify the order of magnitude of the thermal power losses and the resulting temperatures the system without cooling. For that a representative system is modelled and simulated with different load profiles to understand the system behavior and to determine the thermal energy flows. To support the Swissloop team an optimised load profile for the competition will be defined based on new gained knowledge about the system.

To evaluate a cooling system several possible technologies to absorb the heat and transport it from the source to the sink will be discussed. An appropriate heat sink will be evaluated and a high-level design of a possible cooling system will be presented.

1. Modelling a representative system
2. Understanding the system behavior and define the critical design parameters
3. Optimisation of the load profile for the SpaceX Hyperloop Competition 2019 (without cooling)
4. Quantification of the thermal power and energy for a scalable application (Alphatube)
5. Evaluation of the possibilities to absorb heat from the components and transport it to the heat sink
6. Evaluation of a heat sink
7. High-level design of a possible cooling system

Chapter 2
2 System modelling

The aim of the system model is to get a quantitative statement of the heat generation in a Hyperloop pod. Therefore a representative system is modelled with the modelling focus on the heat sources.

2.1 The System (Swissloop Pod 2019)

To be able to quantify the heat sinks and evaluating a cooling system a representative pod system is required. The Swissloop Pod 2019 with name «Claude Nicollier» is used as a reference. The heart of the system is the propulsion unit. It is a completely self-developed linear induction motor (LIM). The basics and the first prototype was designed from the Swissloop alumni Chris Timperio in his master thesis in 2018.[8] Based on this the Swissloop Team developed a second version optimised for their new pod and its ambitions on the competition 2019. The result is a pair of two LIMs with 1.1 meter in length, 5 pole-pitches and 700 Ampere (peak) which are acting together on the aluminium I-Beam of the SpaceX track. There is no contactless suspension or guidance system. For that the pod uses high speed, but low friction wheels. Similar ones were already used in the pod back in 2017 where the team made good experiences with them in creating negligible drag. So the pod is not a Hyperloop concept pod. Nevertheless it is a good pod to test a LIM under Hyperloop conditions. For the braking, the pod uses two brake calipers which are activated by hydraulics, generating frictional force on the track.

The powertrain of this pod is composed of a Battery, an Inverter and finally the two LIMs. The Battery unit consist of two Battery packs in series. Each pack is composed out of 336 Lithium Polymer (LiPo) cells. Where 112 cells are connected in series and 3 of these serial strings in parallel. This is called a 112S3P configuration. The 112 units in series raise the voltage to 450V and the 3 cells in parallel raise the maximum output current to 700 Ampere. That results in a DC power source of 650kW and an energy source of 7.05Ah. In order to generate the necessary altering field in the LIM coils, the DC power is transformed to AC power by 6 high-performance Inverter modules. Two

Component	Picture	technical specifications	critical temperature
LIM	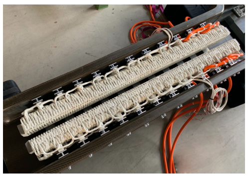	▪ 1.1m in length ▪ 5 pole-pitches ▪ 700A (peak)	insulation: 160°C
Battery	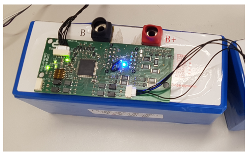	▪ LiPo ▪ 40C ▪ 2.35Ah ▪ 4.2V (max) ▪ configuration: 2x 112S3P	cell: 60°C
Inverter	 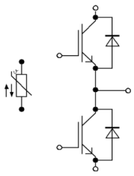	▪ 2x 3 Inverter modules (IGBT, Diode) ▪ 1'700V (peak) ▪ 1'300A (peak)	semiconductor junctions: 150°C
Wheels	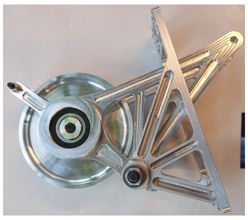	▪ 8x aluminium wheels ▪ 32'800 rpm ▪ angular contact ball bearings	aluminium: ~300°C
Brakes	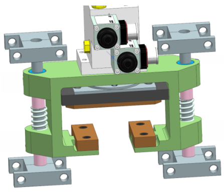	▪ 2x 7000N (resulting braking force) ▪ 0.4 (friction coefficient)	braking-pads: ~500°C

Table 2.1: Components and their specifications for the Pod[9]

times three inverter modules for each phase of each LIM. The mechanical parts of the pod are designed to withstand speeds up to 500 km/h.

2.2 Load profiles

The heat generation of the pod strongly depends on the load profile of the system. Where the load profile of a pod is the targeted trajectory of the pod travelling from A to B. Therefore additionally to a representative system, a representative load profile has to be defined.

Two possible load profiles must be investigated. One that fulfills the criteria of the SpaceX Hyperloop Pod Competition, to accelerate the pod to highest possible speed in the shortest possible distance. And one that fulfills the criteria for a real, full-scale Hyperloop for long-distance transport.

2.2.1 SpaceX Hyperloop Pod Competition

The vacuum tube of SpaceX located in Los Angeles is 1.2km long. For the competition the pod has to accelerate to full-speed and decelerate again without crashing at the end of its 1.2km tube and without damaging the track inside the tube. So the pod has to accelerate as much as possible up to a certain distance that is still far enough away from the end to decelerate the pod to complete standstill. Of course the deceleration will be a full brake with all the power the braking system can provide, to give the pod as much distance as possible for the acceleration process. The acceleration on the other hand has to be as high as possible without destroying any components of the pod or the track.

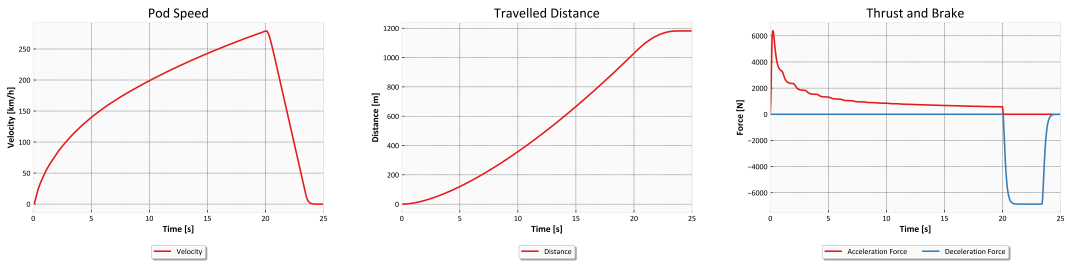

a b c

Figure 2.1: Possible SpaceX load profile

In Fig.2.1 there is a load profile resulting from the model described in Chap. 2.3. For the Battery the ideal model is used (constant voltage Battery). Additionally an infinite cooling on each component is applied to keep them on a constant temperature. The load profile was created by constantly discharging the Battery with 700A. Later it will be shown, what kind of load profile is feasible if the Battery is not ideal and the increase of temperature in the components due to heating losses are not neglected.

For the SpaceX Hyperloop Pod Competition an optimal load profile has to be evaluated, that allows highest speed without cooling and without exceeding the critical temperatures of the components.

2.2.2 Eurotube: Alphatube

The planned vacuum tube of Eurotube located in Collombey-Muraz in the Canton of Valais in Switzerland will have a length of 3km. This is nearly triple the length of the SpaceX vacuum tube. Because it is planned as testing infrastructure, no track should be pre-installed. Therefore there are less limitations for the pod design. Nevertheless, the Swissloop Pod 2019 will continuously serve as a reference system. Hypothetically two possible scenarios should be investigated with the help of this Alphatube.

1. Accelerating the LIM with 1.5m/s2 to 300km/h, then maintaining the speed for the rest of the tube. Full brake at the end.
2. The pod gets accelerated by a induction motor on the track in the first 1km of the tube to 500km/h. The onboard LIM maintains the speed for the rest of the tube before the full brake at the end.

2.3 The Model

2.3.1 Modelica

The development of Modelica started in 1996 with the aim to create a language standard for physical modelling, which should simplify the reuse and exchange of the created models between users. Today Modelica is an object-oriented, equation-based and multi-domain programming language. It is used to create mathematical models of complex natural or man-made physical systems. Especially for dynamic systems where behavior evolves as a function of time.

Most important features of Modelica are:

- It is primarily based on equations instead of assignment statements. This allows more flexibility in the modelling process since equations do not specify a certain data-flow direction. Thus also systems with opposite data-flow direction can be solved without reprogramming

```
//assignment statment
//(one directional; x can be solved)
x := 2 + y;

//equation
//(multi directional; x, y or z can be solved)
x + y = 3 * z;
```

- Consideration of physical units during the solving process. Modelica takes care of the units of the different variables and is able to convert non-SI units thanks to the SIunits-Object of the Modelica Standard Library.

```
SI.Power P=u*i "electrical Power";
```

- It has multi-domain modelling capability. Means that model components correspond to physical objects from several different domains. Each domain specifies a potential- and a flow-variable on which all equations are based on and which allows it to model in a system-physics manner

```
SI.Voltage u "Potential at the pin";
flow SI.Current i "Current flowing into the pin";
```

This differences to conventional programming languages makes Modelica the tool of choice for this modelling task. With Modelica the system to be modelled can be divided into individual subsystems. That makes the model both aesthetically looking and easier to understand.

2.3.2 Model overview

In Fig. 2.2 one can see the top level of the system model. In this graphical representation of the code it is possible to visually see the single components of the model as blocks and how they are connected with each other. The Battery, the Inverter and the LIM introduced in Table 2.1 are seen in this top level view. The brake and the wheels are part of the submodel named «Pod» together with all the other mechanical parts. Different colors of connections represent the different physical domains. Model domains used for this model are given in Table 2.2.

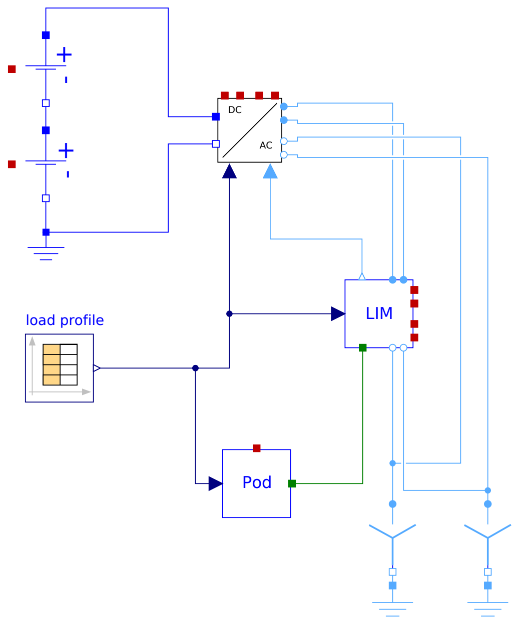

Figure 2.2: Overview of the Swissloop Pod 2019 Modelica model

As input for the simulation there is a table named «load profile», in which the pod velocities for different simulation times can be predefined. With the mass of the pod and its resistance forces a necessary thrust force is calculated in order to meet the required speed. The LIM submodel will determine the AC current, that must flow through the LIM coils to deliver the necessary thrust. Out of the velocity and the current, all the values of the components in the AC circuit are derived inside the LIM submodel. In order to get the values for the DC circuit and finally for the Batteries, an energy balance over the Inverter is solved. All the electrical power consumed in the AC circuit plus all the energy losses inside the Inverter has to be delivered from the DC circuit. The Batteries will provide a certain voltage depending on the charge of the Battery. Since the DC power is defined as $P_{DC} = U \cdot I$ and provided by the Batteries, the DC current can directly be calculated. Out of that all the remaining unknown values in the DC circuit can be estimated.

color	path	typical components	potential variable	flow variable	additional variables
green	Mechanics. Translational	mass, forces, spring/damper, frictional elements, elastogaps	position, s [m]	force, f [N]	-
blue	Electrical. Analog	resistor, conductor, inductor, diode, NPN, PNP, voltage/current source	voltage, v [V]	current, i [A]	-
light blue	Electrical. QuasiStationary. MultiPhase	same as Electrical.Analog but only for AC (sinus signals)	complex voltage, v* [V]	complex current, i* [A]	angular vel. of ref. frame, omega [rad/s]
red	Thermal. HeatTransfer	heat capacitor, thermal resistor, convection, radiation	temperature, T [K]	heat flow rate, Q_flow [W]	-
dark blue	Blocks	functions, integrator, derivative, filter, logic, limiter, tables,...	type real	-	type boolean, type integer

Table 2.2: modelling domains and its components and variables used in the model

The model was designed with the focus on heat sources. Therefore the modelling depth of the electric circuits, especially on the AC side, was kept on a low level. That is why all transient effects are neglected and the quasi stationary approach was chosen. The LIM submodel forms the core of the model and is based on a 3D COMSOL model of the LIM, which comes from the work of Chris Timperio [8]. Thus, the results of the system model are strongly dependent on that COMSOL model. In the following section the modelling of the individual submodels will be discussed in more detail.

2.3.3 Components

Battery

The Battery is the only power source of the pod. Three different Battery models are used. The most simple one is the ConstantVoltage source model from the Modelica standard library (MSL) named ideal Battery. The advantage of this model is, that the Battery will never be unloaded and can provide infinite current. This will be helpful for some case study's.

The ConstantVoltage source is a simple source for an ideal constant voltage which is provided by a parameter. There is no internal resistance modelled. If it is used instead of a Battery model it is not very realistic: This Battery will never be unloaded.[10]

A more advanced model is given in Fig. 2.3. Here the Battery is modelled as a circuit of several serial and parallel cells. The number of parallel and serial cells is provided by input parameters. Each cell is considered as a series of a ConstantVoltage source and a Resistor both from the standard Modelica library. The Resistor is able to transform the electrical energy losses into heat. The heat produced in the resistor is connected to two thermal masses. One is representing the mass of the materials used for the galvanic cell and the other is the mass of the material surrounding the cell - mostly Silica gel is used for that purpose. The thermal mass of the cell material is assumed as 3/4 of the mass of the cell. The rest is Silica gel. In this model the Battery will still never be unloaded but the discharging current is limited by the internal resistance.

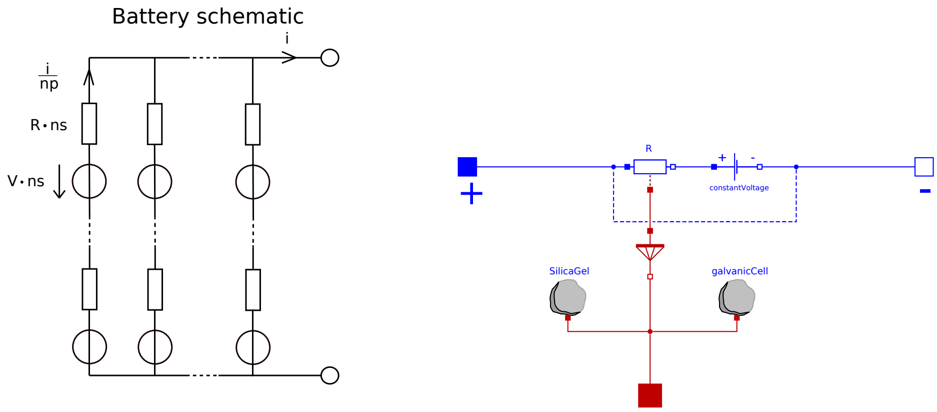

a b

Figure 2.3: Battery submodel, schematic (a) and implementation (b)

The third and most advanced Battery model is a model from the ElectricalEnergyStorage (EES) Library (Path: EES.Batteries.Stacks.Basic.StaticResistanceScaled). It is also modelled as a circuit of several serial and parallel cells. Each cell is considered as a series of a voltage source and a resistor. For the estimation of the voltage provided by the voltage source, a state of charge (SOC) vs. open circuit voltage (OCV) table is implemented. That allows the model to adapt the provided voltage to its actual charging level of the cell. This results in a more realistic representation of the Battery and point out the limits of possible total energy consumption in the pod.

In Fig. 2.4 the three different Battery models are compared with each other. In a simple test configuration the Battery models are connected to an electric load, that requests more and more energy over time from the Battery. The different reality depths of the models can be seen clearly. The ideal ConstantVoltage model (red) offers more and more current without loosing voltage. The more advanced model (green) loses voltage because of the losses in the internal resistance and therefore has to provide more current to overcome that losses. The most advanced model (blue) collapses at some point in time, where the voltage drops to minus infinity, because the SOC is reaching zero. Thus the simulations with that model will always fail at some point, if the load consumes more energy then available in the Battery.

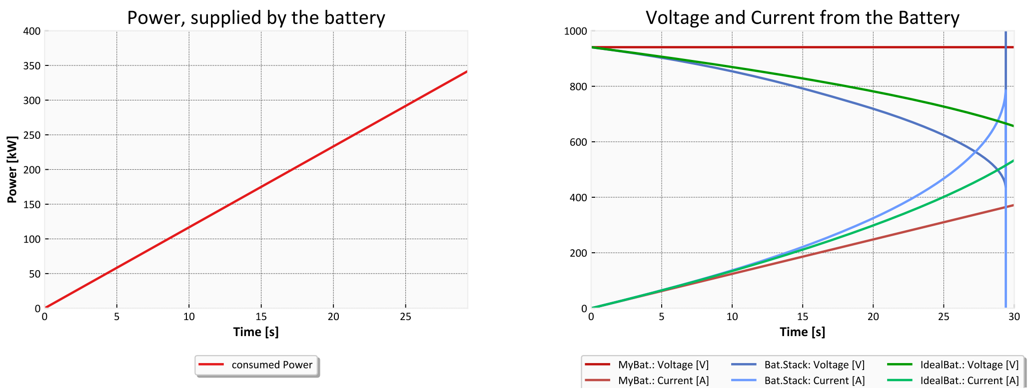

a b

Figure 2.4: Three different Battery models in direct comparison

To validate the implemented more advanced Battery model, given in Fig. 2.3 a simple resistance load is connected to the Battery. Two Battery variants with different cell configurations (number of serial and parallel cells) are tested. As seen in Fig. 2.5 the two tested variants offer the amount of current which was predicted by the hand calculation. Therefore it can be assumed that the serial and parallel configuration is correctly implemented and the Battery model will behave as expected.

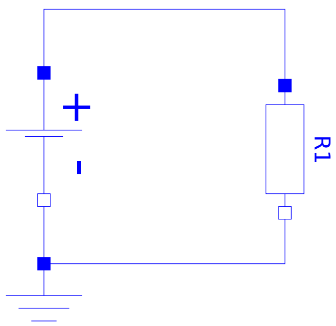

U_{cell}	$10\,V$	cell voltage	Variant 1: $n_p = 3; n_s = 1$ $U_{Bat} = U_{cell}$ $R_{ges} = \frac{1}{3 \cdot \frac{1}{R_{cell}}} + R_1$ $I = 9.68\,A$
R_{cell}	$0.1\,\Omega$	cell inner resistance	
R_1	$1\,\Omega$	load resistance	
n_p	-	numb. cells in parallel	Variant 2: $n_p = 1; n_s = 3$ $U_{Bat} = 3 \cdot U_{cell}$ $R_{ges} = 3 \cdot R_{cell} + R_1$ $I = 23.08\,A$
n_s	-	numb. cells in series	
$I = \frac{U_{Bat}}{R_{ges}}$			

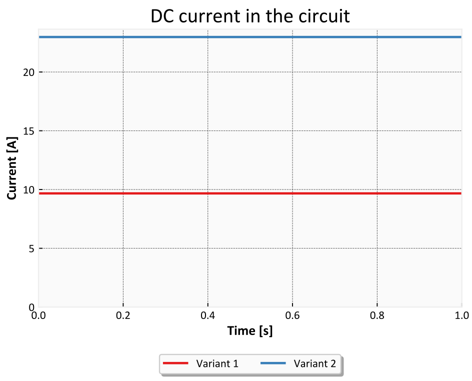

Figure 2.5: Validation of the Battery submodel with two variants

Inverter

The Inverter is implemented as a black box. So the components of the Inverter like resistances, diodes, transistors, etc. are not modelled. The Inverter follows exclusively the energy conservation. The power consumed on the AC side and the losses produced by the Inverter itself has to be the same as the power provided on the DC side. Since there are two sides of the LIM with 3 phases each, the Inverter has to provide 6 phases with the necessary power, requesting the power from the DC side.

$$P_{DC} = \sum_{3Phases} P_{AC_1} + \sum_{3Phases} P_{AC_2} + \dot{Q}_{th}$$

Each phase has its own voltage source from the Electrical.QuasiStationary.MultiPhase model domain. In this model domain all components are stacked according to the number of phases. That is why in Fig. 2.6 only two voltage sources are seen, even there are six modelled. The value of the complex voltage they have to provide is evaluated by the LIM model. The only load attached to the source is the LIM and therefore the voltage drop over the LIM has to be balanced out by the AC source of the Inverter. The frequency of the voltage source is determined by the results of the already mentioned COMSOL model of the LIM. It provides the information for which pod velocity which electric frequency generates the most mechanical power in the LIM. This frequency will be chosen by the Inverter.

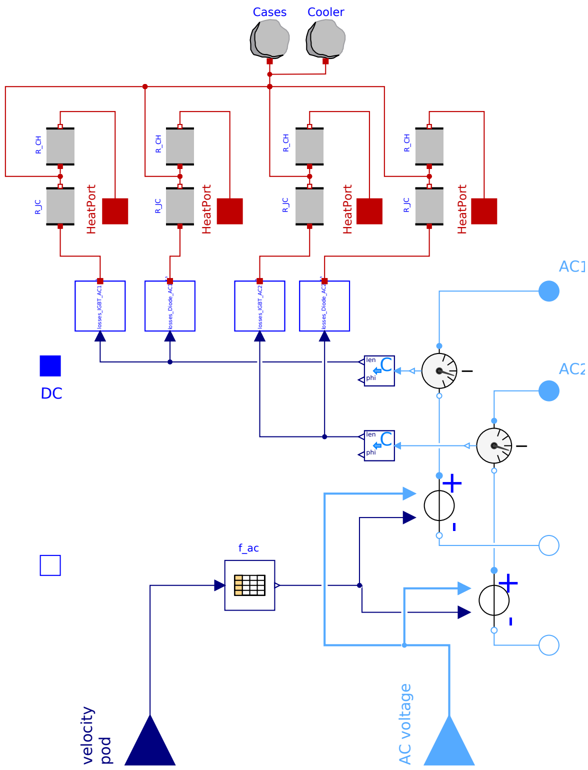

Figure 2.6: Inverter submodel implementation

With the currents flowing in each phase, the losses of the IGBT transistor and the diode are determined with the values from the datasheet of the Inverter module. The transistor as well as the diode are producing heat because of the switching losses in the semiconductor junctions as well as joule losses in the deduced resistance of the semiconductor material. Fig. 2.7a shows the energy loss of one switch-on and one switch-off process depending on the AC current and the temperature of the junction. Fig. 2.7c is the same for the diode with one difference - the diode produce losses only once per switch instead of two. Fig. 2.7b and d shows the voltage drop over the internal resistance of the junction depending on the temperature of the junction for the transistor and the diode. Because the temperature dependence of the resistance of the junction generates numerical problems and the fact that the change in value is relatively small, a constant temperature of 50°C is assumed for the joule losses.

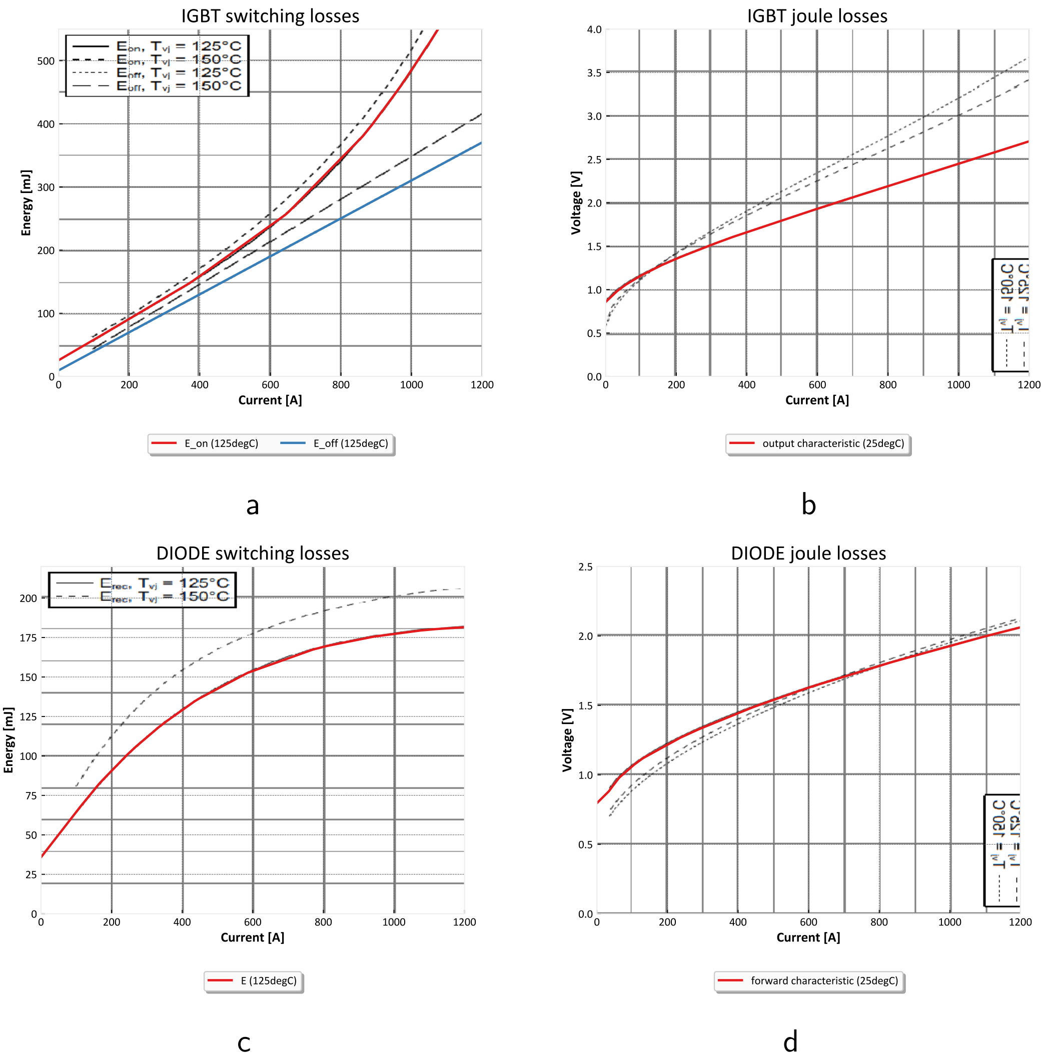

Figure 2.7: Inverter losses validation by compairing with the datasheet

In order to get the temperature of the Inverter, thermal resistances are implemented. The resistances are given in the datasheet. There is a resistance «junction to case» and «case to heat sink». The cases of all 6 modules are modelled as one thermal mass of 1kg of iron. The other thermal mass is the model for the aluminium block which acts as a cooler for the Inverter modules. It is modelled as 6,74kg of aluminium. Because of numerical reasons it is added before the «case to heat sink» resistance. This will cause a minimal error in the temperature results which will be taken into account. With that the temperatures in the junctions as well as at the heat conducting surface on the case can be observed in the simulations.

Linear induction motor

As already mentioned the LIM submodel is the core of the whole model and is based on a 3D COMSOL model. See also Chap. 2.3.2. The schematic for the model of one side of the LIM is given in Fig. 2.8a. It is just as simple as a Y-connection with a deduced resistance and an ideal coil in series for each phase. Where the values of the coils and resistances are dependent on the AC current flowing through the components and the velocity of the pod. This dependency is given by the lookup tables «Table_R» and «Table_L». The current which has to go through the AC phases is evaluated using a lookup table which delivers values for the thrust produced by the LIM depending on the velocity of the pod and the current flowing through the LIM coils. This lookup table named «Table_F» is the most important piece of the LIM model because it covers the physics of how this motor is converting electrical to mechanical energy depending on the rotor speed (pod velocity). Two more lookup tables are «Table_Ur» and «Table_Ui». This tables define the voltage drop over the LIM and serve therefore as the information for the complex voltage delivered by the Inverter as discussed in Chap. 2.3.3. The last table which is given in Fig. 2.8b is named «Table_B» and contains a rough estimation of the B-Field values inside the LIM core, estimated grafically out of colormap plots from the COMSOL model.

All these lookup tables are filled with results from simulations of the mentioned COMSOL model and are used to get values for the modelled parts of the LIM. They all depend on the actual current and pod velocity. To get an idea of how the COMSOL model works and the theory behind that, the master thesis of Chris Timperio [8] hold the answers.

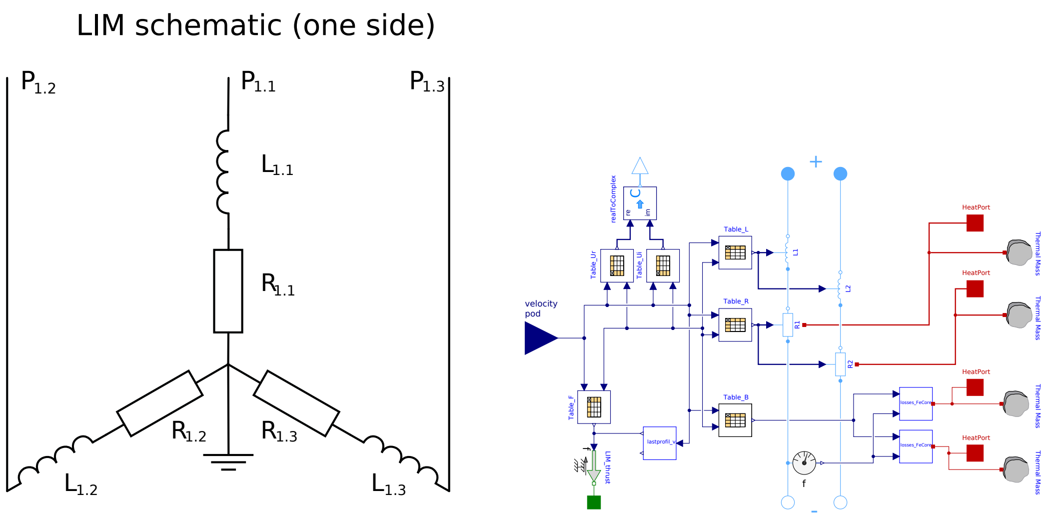

a b

Figure 2.8: LIM submodel, schematic (a) and implementation (b)

Two heat sources are modelled in the LIM submodel. One is the joule heating inside the deduced resistances. The formula to cover joule heating inside induction motor coils is given by

$$P_{th} = R(T) \cdot I_{RMS}^2$$

With that formula all the possible effects of heating inside LIM coils are considered to generate heat. Another heat source in the LIM are the iron losses in the core. The formula to rough estimate the iron losses is given by

$$P_{th} = m_{Fe} \cdot v_{1.5T} \cdot \left(\frac{B}{1.5T}\right)^2 \cdot \left(\frac{f_{AC}}{50Hz}\right)^{1.6} \cdot k_B$$

m_{FE}	$16.6\,kg$	iron mass of the core
$v_{1.5T}$	$1.1\,\frac{W}{kg}$	specific losses at 50Hz and 1.5T
B	«Table_B»	B-Field in the core
f_{AC}		frequency of the AC current
k_B	1.3	manufacturing coefficient

[11]

The core as well as the coils are modelled as thermal masses which will heat up during run. For the coils 8.5kg of copper for each side is considered as thermal mass. The core is considered to be 16.6kg of iron. Heat is able to flow between the copper coils and the iron. Therefore a thermal resistance between the thermal masses with a thermal contact number of $20\frac{m^2 \cdot K}{W}$ and a thermal contact surface of $0.0762m^2$ was added. The thermal contact number is roughly estimated with the Table 2.3a.

Thermal Resistance, $R''_{t,c} \times 10^4$ (m$^2 \cdot$ K/W)				
***(a)* Vacuum Interface**			***(b)* Interfacial Fluid**	
Contact pressure	100 kN/m^2	10,000 kN/m^2	Air	2.75
Stainless steel	6–25	0.7–4.0	Helium	1.05
Copper	1–10	0.1–0.5	Hydrogen	0.720
Magnesium	1.5–3.5	0.2–0.4	Silicone oil	0.525
Aluminum	1.5–5.0	0.2–0.4	Glycerine	0.265

Table 2.3: Thermal contact resistance for (a) metallic interfaces under vacuum conditions [12]

The validation only checks the modelling of the heat sources. The modelling of the electrical part and therefore the results from the COMSOL model is assumed to be correct. For the validation a constant current of 300 Ampere (RMS) is flowing through the coils for 10 seconds. The coil temperature will be observed and compared with a hand calculation.

$J = \frac{I_{RMS}}{A} = 23.8 \cdot 10^6 \, \frac{A}{m^2}$	I_{RMS}	$300 \, A$	active current
	A	$1.26 \cdot 10^{-5} \, m^2$	cross section
$\Delta T_{Coil} = \frac{J^2 \cdot \rho_R \cdot t}{C \cdot \rho_m} = 27.6 \, K$	t	$10 \, s$	time
	ρ_R	$1.68 \cdot 10^{-8} \, \Omega m$	resistivity of copper
	ρ_m	$8'960 \, \frac{kg}{m^3}$	density of copper
	C	$385 \, \frac{J}{kg \cdot K}$	specific heat capacity of copper

The result of the validation simulation is shown in Fig. 2.9. The resulting temperature change is much higher in the simulation than in the hand calculation. The simulation gives a change in temperature of about 120°K while the hand calculation gets 30°K temperature change. Nevertheless, the model is rated as correct. Because the hand calculation assumes constant resistance of the copper during the whole 10 seconds. But it can be seen in Fig. 2.9d that the resistivity of the copper changes drastically over time.

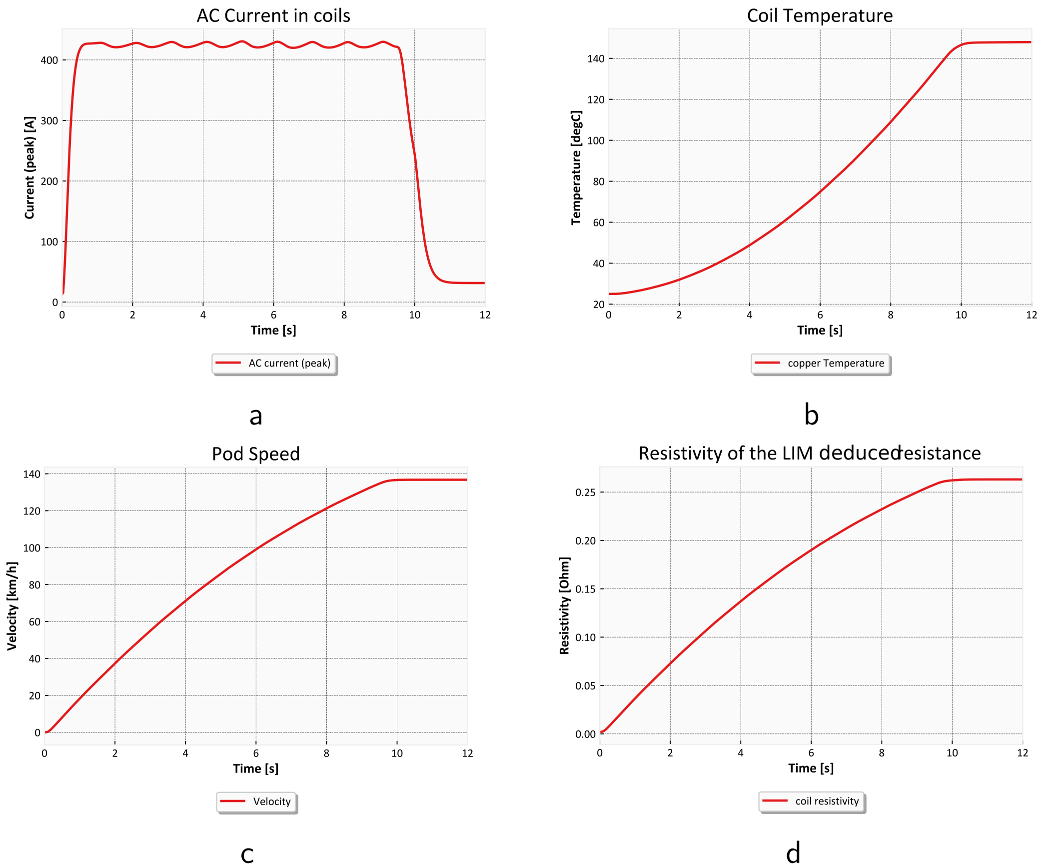

Figure 2.9: Validation of the LIM heat source

There are two effects which influence the resistance of the copper. On one hand there is a temperature dependency of the resistance whose effects are not negligible. And on the other hand a linear relation between the pod speed and the copper resistivity can be observed. That is related to an effect named backEMF. It is an induces voltage inside the coils which acts against the external voltage drop. This effect is reflected in a smaller voltage drop over the motor which increases with velocity. Because the current is forced to be constant in that scenario the deduced inner resistance will rise with velocity.

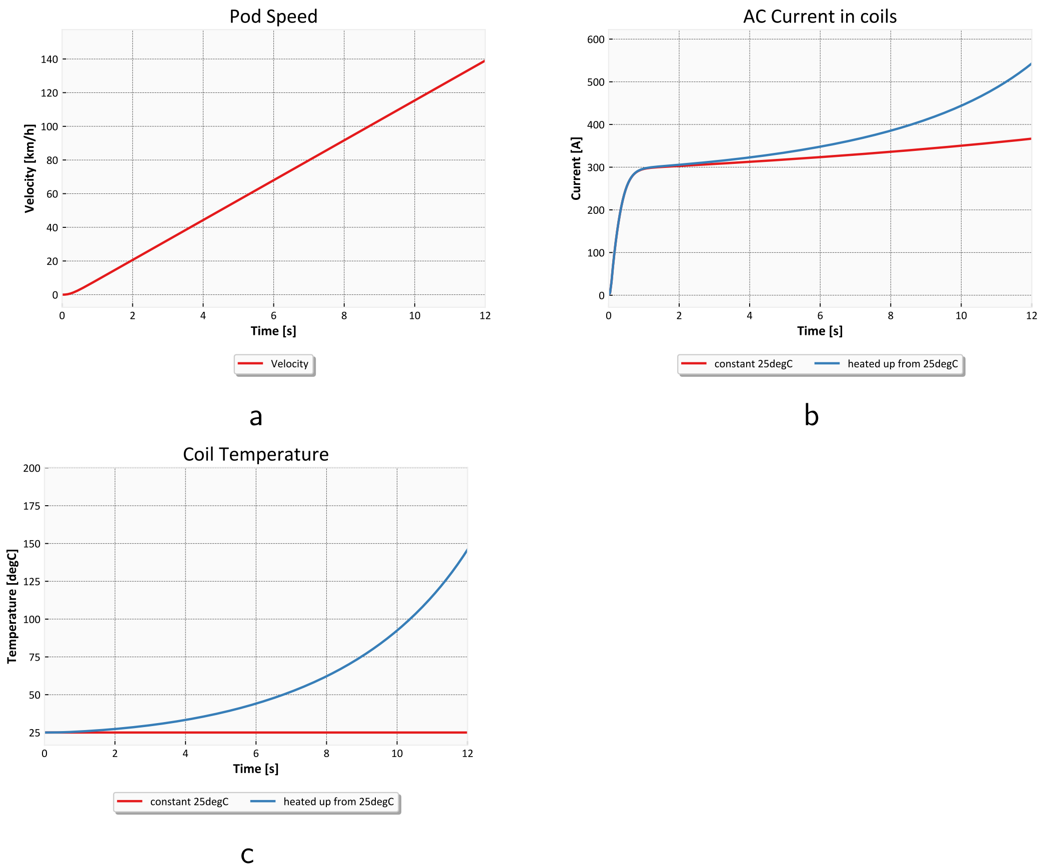

Figure 2.10: Effect of pod velocity and LIM temperature on LIM performance. Constant thrust of 1000N

The value of the AC current trough the coils at constant acceleration and therefore constant thrust force shows the behavior of the LIM at different speeds very well. In Fig. 2.10 two simulations at constant 1000N thrust were run. The simulations were done once with an infinitely good cooling which keeps the coils always at 25°C (red curve) and once without cooling (blue curve). By just looking at the red, cooled simulation it is seen that the current rises with speed. This means that with increasing speed more current is needed to maintain the required constant thrust.This effect of losses in linear motors with short stator is called end effects and the reason why long stators usually make the run. The longer the stator, the smaller the end effects. The value of the losses due to end effects at a speed of 90km/h are the same as the value of the losses due to the rise in temperature of 100°C. That tells us that the second limiting design parameter of a LIM besides the end effects is the generating heat inside the coils. To conclude, a LIM loses his initial good efficiency with increasing speed due to the end effects and with increasing temperature due to the joule heating.

Vehicle

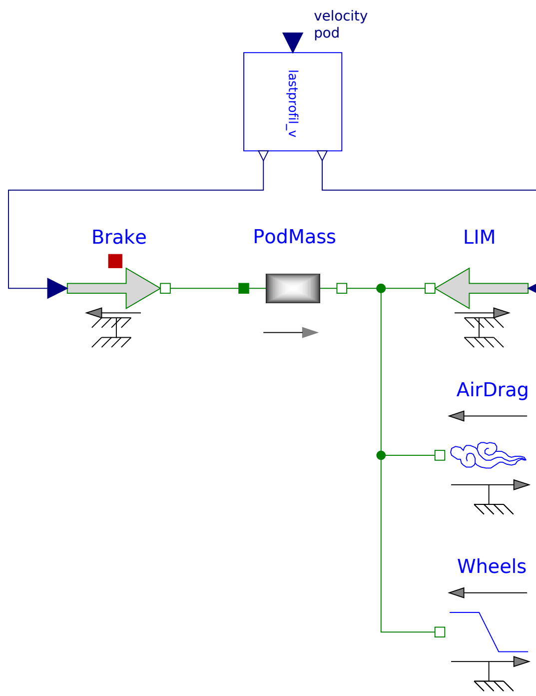

Figure 2.11: Vehicle submodel implementation

The vehicle or «Pod» submodel covers all mechanical parts of the system. It is using the Mechanics.Translational modelling domain of the MSL library. The core of that submodel forms the PodMass on which all relevant mechanical forces act. The podmass represents the whole mass of the pod or the complete mass that needs to be moved. As seen in Fig. 2.11 there are four forces modelled acting on the podmass. The LIM provides the thrust for the acceleration and the brake for the deceleration. The air drag and the friction of the wheels are the mechanical resistances acting on the mass. Together, they determine the trajectory that the vehicle will make. The implemented physics for that is newton's law of motion:

$\sum F = m_{pod} \cdot a$	$\sum F$		sum of all forces acting on the pod mass
	m_{pod}	$300\,kg$	mass of the pod
	a		acceleration/deceleration
$a = \frac{dv}{dt} = \frac{d^2s}{dt^2}$	v		velocity (load profile)
	s		traveled distance
	t		time

For the validation a simple load profile (1s acceleration, 1s keeping speed, 1s deceleration) at a 100kg vehicle which gets accelerated to 3m/s is used. A hand calculation and a simulation with the submodel are compared.

$$F_{acc} = m \cdot \frac{v_{max}}{t} = 300N$$

$$F_{roll} = \mu \cdot m \cdot g \cdot n = 11.8N$$

$$F_{drag} = c_w \cdot A \cdot \rho_m \cdot \frac{v_{max}^2}{2} = 0.0022N$$

m	$100\,kg$	vehicle mass
v_{max}	$3\,m/s$	target vehicle speed
t	$1\,s$	acceleration time
μ_R	0.0015	rolling resistance coefficient
g	$9.81\,\frac{m}{s^2}$	gravitational acceleration
n	8	number of wheels
c_w	0.12	drag coefficient
A	$0.386\,m^2$	cross-sectional area (perpendicular to the flow)
ρ_m	$1.0343 \cdot 10^{-2}\,\frac{kg}{m^3}$	density of air (900Pa,30°C)

As seen in Fig. 2.12 the results of the simulation are close to exactly the same as the hand calculations have predicted. Therefore the submodel is rated as correct.

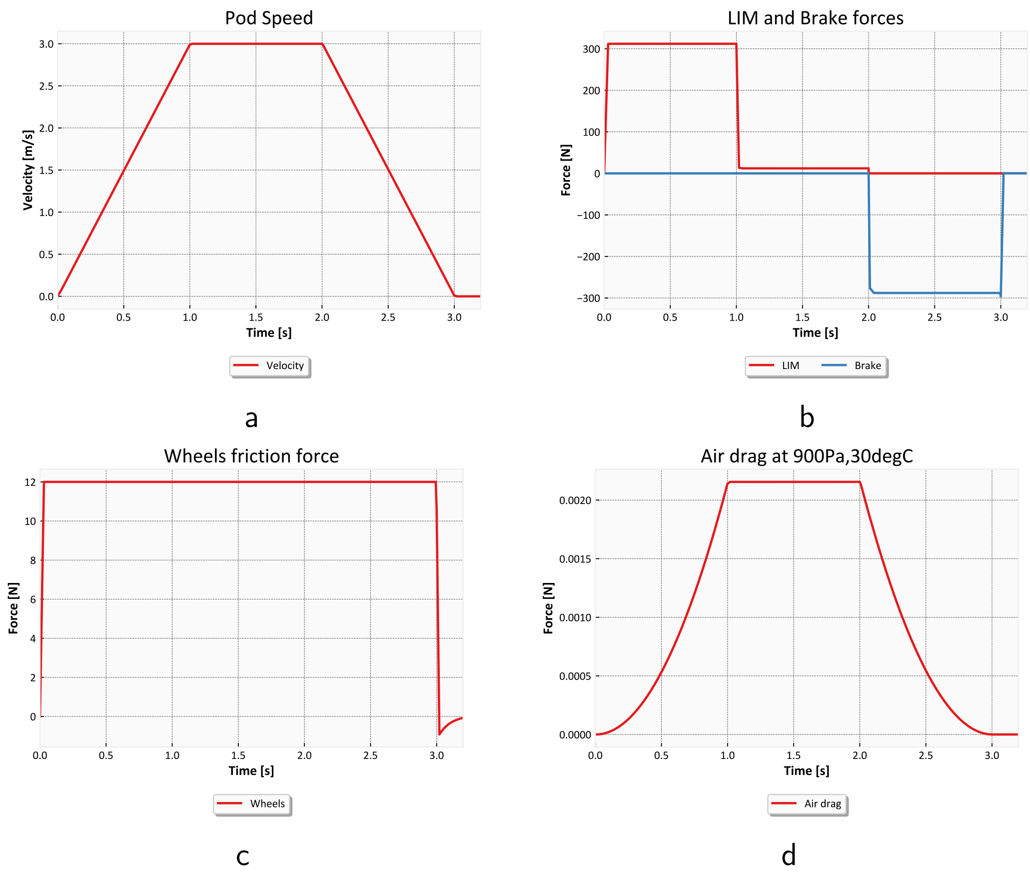

Figure 2.12: Validation of the vehicle submodel with a 100kg vehicle

2.4 Conclusions

The created system model of the Swissloop Pod 2019 is able to show some interesting system behavior with regard to thermal losses and temperatures of the components. In Fig. 2.13 one can see a simulation of the system model with the most advanced Battery submodel. The model variant that predicts the reality best. No cooling is applied. The applied load profile for the simulation is shown in Fig. 2.13a. The pod is accelerated for 12s with constant 1000N force (similar to the simulation in 2.10). Then it is decelerated with 7000N which corresponds to full braking. In Fig. 2.13b-d the resulting temperatures respectively thermal power due to losses during the run are shown. None of the components exceeds its critical temperatures of Table 2.1. Nevertheless, the power losses of the Battery and the LIM become very high with increasing component temperature and speed.

The Inverter produces a base load of thermal losses of about 10kW just to generate the AC current. This base load also changes slightly with temperature which is related to the temperature dependent switching losses of the semiconductors. Actually it starts at 8.5kW and increases until 12 seconds to 13.5kW.

Fig. 2.13f shows the shares of the individual components to the total thermal power losses. 100% is corresponding to the total amount of thermal power loss shown in Fig. 2.13c. The plot shows at what state of the run which component is how much responsible for the incurred losses. It is interesting to consider the time range from 0 to 12 seconds where the pod is accelerating. At first the Inverter is the most relevant heat source until a current density in the LIM coils of 15 A/mm2 is reached. At that point the LIM replaces the Inverter as the most relevant heat source. This holds on until 12 seconds where the current density exceeds 25A/mm2. From that point on, the Battery became the most relevant heat source for the rest of the run until braking.

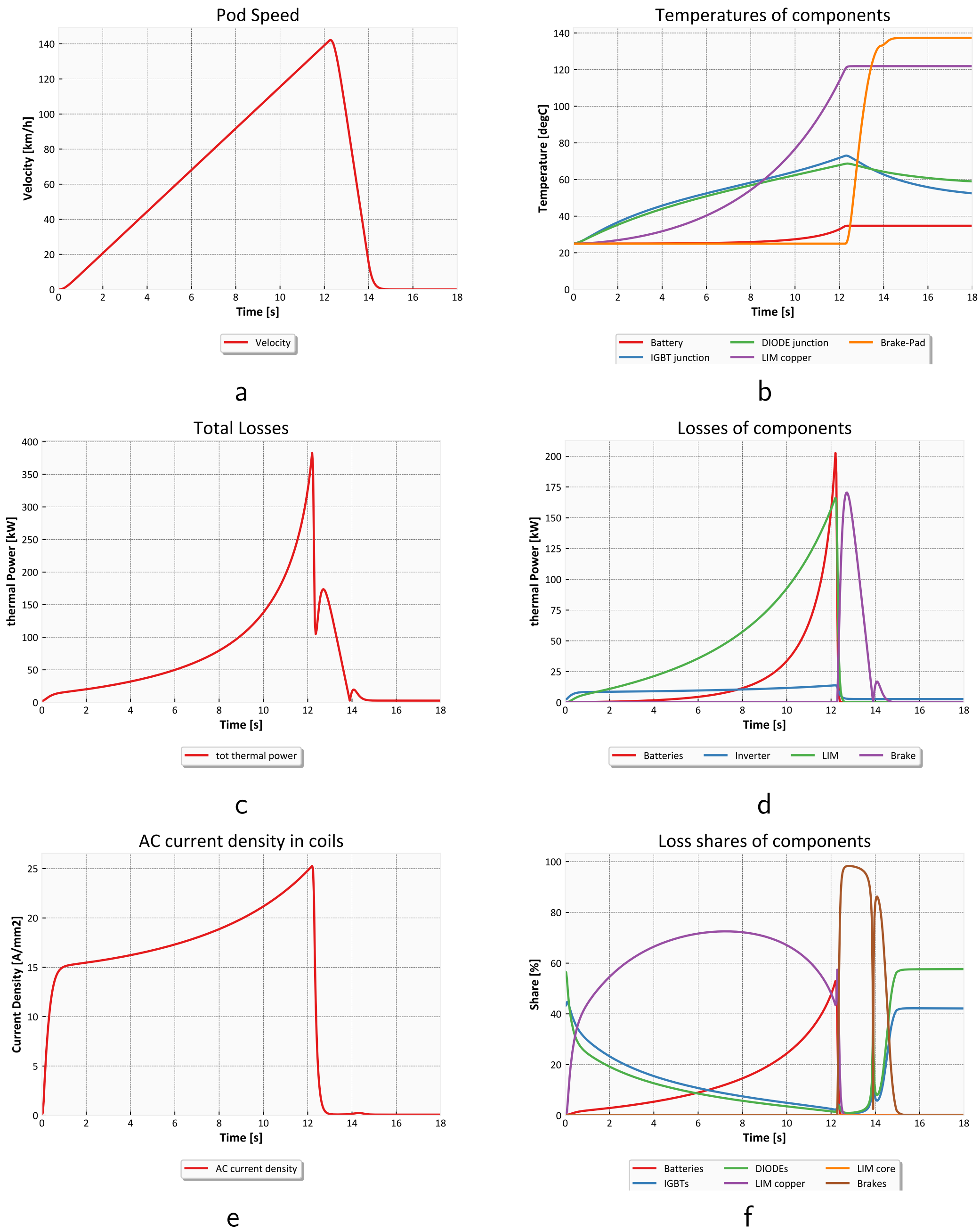

Figure 2.13: Temperatures and losses with a load profile resulting constant thrust of 1000N for 12s and a brake force of 7000N

Therefore the two most critical components in terms of power losses are the LIM coils and the Batteries. In both components, joule heating is the essential heat source. With increasing speed the LIM consumes more current which results in more joule heating and a rise in temperature inside the copper. With the rise in temperature, the LIM consumes even more current. If the LIM consumes more power, the Battery has to deliver more power too. The voltage of the Battery is given by the SOC of the cells and therefore unchangeable at this moment. To deliver more power the discharge current of the Battery has to rise. The Battery also suffers from joule heating that is why the temperature of the cells will rise which results in an even higher discharging current. Additionally the voltage of the Battery will fall during run because of discharging. This again results in an increase in discharging current from the Battery.

The rise of temperature in electrical components suffering from joule heating is a vicious circle that must be interrupted by effective cooling to be able to drive longer distances with such kind of system.

In order to find the most efficient operating point of the powertrain (Battery-Inverter-LIM-Movement) the pod efficiencies of an non-cooled model at different constant thrusts are plotted against the pod velocity. The result can be seen in Fig. 2.14a. At very low speeds high Thrusts are most efficient. But this is only true up to a speed of 13km/h. At this point the thrust has to be reduced step by step to 750N at 27km/h. With that Trust the powertrain reaches its maximum efficiency at 50km/h and has a value of 19.4%. For faster speeds the efficiency falls again. At 90km/h the 500N thrust takes over the efficiency leadership and at 175km/h the 50N thrust is best.

$$\mu_{pod} = \frac{v_{pod} \cdot F_{LIM}}{P_{el,Battery} + \dot{Q}_{th,Battery}}$$

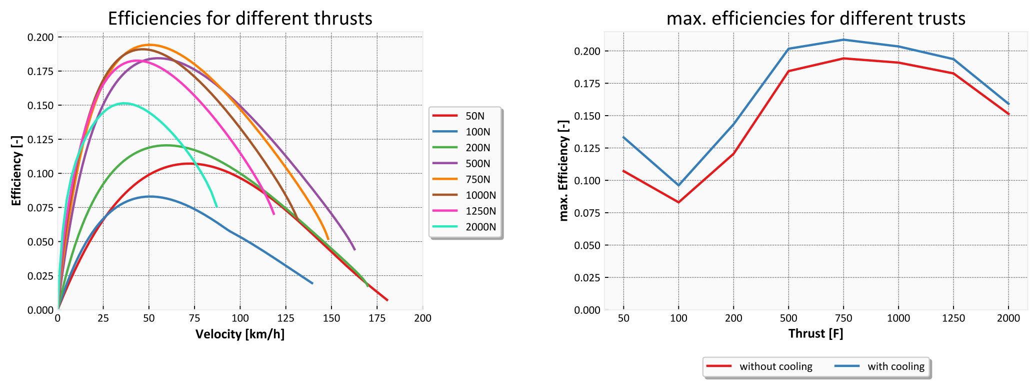

a b

Figure 2.14: Powertrain efficiency of the modelled pod. (a): different efficiencies without cooling. (b): peak efficiencies with and without cooling

In Fig. 2.14b, the efficiency peak point of every constant thrust curve from a is plotted. Ones without cooling like in a (red curve) and ones with an ideal cooling applied (blue) which keeps all the components always at 25°C. One can see that the peak efficiencies increases for all thrusts applied. Especially the low thrusts profit from the cooling system. Out of that it can be concluded that temperature is the most relevant effect that reduces efficiency at low thrusts while at high thrusts the end effects of the LIM are more relevant and cooling is less profitable.

Chapter 3

Cooling concept

Now that we know the system behavior and have a reliable model it is time to evaluate a cooling system suitable for Hyperloop systems.

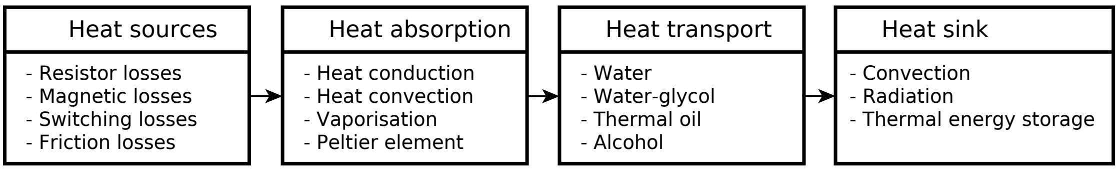

Figure 3.1: Schematic of the cooling concept

3.1 Heat sources

3.1.1 Physical mechanisms

The main physical mechanisms for thermal heat production in a LIM powered Hyperloop pod are listed below:

Kind of losses	Where to find in our system	Where to find in the model
Resistor losses	Battery, Wiring, LIM coils, Semiconductors, PCBs, etc.	Battery, LIM coils, Inverter
Magnetic losses	LIM coil, LIM core, Magnetisable metals	LIM core
Switching losses	Semiconductors, Microcontrollers	Inverter
Friciton losses	Wheels, Brakes, Shell	Brake

Table 3.1: Heat producing mechanisms found in the system and modelled

As given in Table 3.1 lots of heat source are neglected because they are assumed to be very small compared to the others. Following, the individual mechanisms and its physical and mathematical description are explained.

Resistor losses

Heat is generated in each conductor through which electricity flows. This physical mechanism is known under the name «ohmic heating», «resistive heating» or «joule heating». In the following joule heating is used as the name for this mechanism, because of Joule's first law: The power of heating generated by an electrical conductor is proportional to the product of its resistance and the square of the current.

DC side: $$P_{th} = I \cdot U(T) = I^2 \cdot R(T)$$	I	A	DC current
	$R(T)$	Ω	active resistance
	U	V	DC voltage
	$i(t)$	A	AC current
AC side: $$P_{th}(t) = i(t) \cdot u(t,T)$$	$u(t)$	V	AC voltage
Quasi-Stationary approach: $$\begin{aligned} P_{th,avg} &= Re(conj(i^*) \cdot u^*) \\ &= I_{RMS}^2 \cdot Re(Z(T)) \end{aligned}$$	i^*	A	complex current
	u^*	V	complex voltage
LIM: $$P_{th.avg,LIM} = I_{RMS}^2 \cdot R(T)$$	I_{RMS}	A	average active current
	$Z(T)$	Ω	complex impedance
$$R(T) = R_{ref} \cdot [1 + \alpha_{ref}(T - T_{ref})]$$	R_{ref}	Ω	Resistance at reference temperature
	α_{ref}	-	linear temperature coefficient

The thermal power losses due to joule heating on the DC side is rather simple. It is the product of current and voltage. For alternating signals the product has to be taken at every step in time so the resulting power would also be an alternating signal. Since the model uses the quasi stationary approach an averaged power loss is easily calculated using the complex current and voltage.

For the joule loss in the LIM this «normal» approach with the complex numbers is not valid. Because of the effect of backEMF discussed in Chap. 2.3.3 the voltage drop over the motor does not give the correct result. But the version with the average active current will correctly reproduce the physical effects in the motor.

The active resistance of every electrical resistor depends on the temperature of the resistor material. This temperature dependency is mostly modelled as linear with a temperature coefficient. This description of the temperature dependence of the resistive material is very accurate and widely used.

Magnetic losses

There are two main physical mechanisms primarily contribute to the magnetic losses. These are hysteresis losses due to changes in the magnetisation and induced eddy-currents in the involved materials. Because the losses are dependent to the permeability of the materials the losses in copper can be neglected. The other mainly involved material is the iron core of the LIM which is made of electrical steel (M 270-35 A). For such fully-processed electrical steel the magnetic properties are guaranteed. According to [11], the following properties are given for M 270-35 A:

name	density	max. losses at 50 Hz and 1,5T (benchmark)	max. losses at 50 Hz and 1,5T (guaranteed)	min. polarisation at 5,000 A/m (guaranteed)	max. anisotropy of loss (+/-) (guaranteed)	min. bending coefficient (guaranteed)
M 270-35 A	7,65 kg/dm3	1,1 W/kg	2,7 W/kg	1,6 T	17 %	2

Table 3.2: properties of M 270-35 A electrical steel[11]

With that properties and the following equation, the thermal power loss in the LIM core can be roughly evaluated. As given in Fig. 2.13e the magnetic losses are negligibly small, which is why a more precise modelling of these losses will not be made.

$$P_{th} = m_{Fe} \cdot v_{1.5T} \cdot \left(\frac{B}{1.5T}\right)^2 \cdot \left(\frac{f_{AC}}{50Hz}\right)^{1.6} \cdot k_B$$

m_{FE}	kg	mass of the electrical steel
$v_{1.5T}$	$\frac{W}{kg}$	specific losses at 50Hz and 1.5T
B	T	B-Field in the core
f_{AC}	Hz	frequency of the AC current
k_B	-	manufacturing coefficient

[11]

Semiconductor switching losses

In power electronics the transformation of the electrical signal is done by chopping and smart switching of the input signal. This is mainly done by semiconductor devices like transistors and diodes. The mechanism behind semiconductor physics is the junction between different doped semiconductor materials. During the switching process the space charge region in the junction gets rearranged which produces heat. The switching losses of an Inverter module composed of one IGBT transistor and one diode is calculated by

$P_{th} = (E_{t,on} + E_{t,off} + E_{d,rec}) \cdot f_{switch}$	f_{switch}	Hz	switching frequency
	$E_{t,on}$	J	switching-on losses transistor
	$E_{t,off}$	J	switching-of losses transistor
	$E_{d,rec}$	J	switching losses diode

The values for the switching energy losses are provided by the datasheet of the Inverter module. See Fig. 2.7

Friction losses

There are different types of friction losses present in the pod. Sliding friction in the braking pads, rolling friction in the guiding and suspension wheels and air drag on the outer shell acting with the surrounding fluid. The thermal power loss due to friction is given by

$$P_{th} = F_{friction} \cdot v$$

By comparing the equations for the different types of friction, it can be seen that the order of magnitude in terms of resulting thermal power of rolling friction and air drag is negligibly small. In fact the power is too low to let the component material increase temperature noticeably. Therefore these heat sources are neglected in the further considerations.

$F_{slide} = \mu_{slide} \cdot m \cdot g$	m	kg	vehicle mass
	μ_{slide}	~ 0.4	sliding friction coefficient
	μ_{roll}	~ 0.001	rolling resistance coefficient
$F_{roll} = \mu_{roll} \cdot m \cdot g$	g	$9.81\,\frac{m}{s^2}$	gravitational acceleration
	v	m/s	vehicle velocity
	c_w	~ 0.1	drag coefficient of the vehicle
$F_{drag} = c_w \cdot A \cdot \rho_m \cdot \frac{v^2}{2}$	A	$\sim 0.5\,m^2$	cross-sectional area of the vehicle (perpendicular to the flow)
	ρ_m	$1.0343 \cdot 10^{-2}\,\frac{kg}{m^3}$	density of air (900Pa,30°C)

3.1.2 Load profile «SpaceX»

The aim of the SpaceX load profile is to reach highest speed within the 1.2km tube of SpaceX without damaging the pod nor the track. The intention of the Swissloop team was to achieve this by providing maximum possible current out of the Battery to the LIM. This would be 700 Ampere DC output. If this would work, very high speeds would be possible in a very short acceleration distance.

In Fig. 3.2 this scenario was simulated (red curve). After 5 seconds the Battery reaches its critical temperature of 60°C. And the LIM coils will reach its critical temperature of 160°C after 6 seconds. This shows, that even if the electrical components could manage to provide such high currents, the components would fail after a few seconds because of overheating.

With the knowledge won in Chap. 2.4, some optimised load profiles were made. The most interesting ones are given in Fig. 3.2. The first improvement was done by reducing the current provided by the Battery drastically after 2 seconds from 700 Ampere down to 200 Ampere and completely turned off the motor after 13 seconds. With that change on one hand the maximum velocity came down to 138 km/h. But on the other hand all the components now remain below their critical temperatures. Only the LIM will heat up to 180°C, which should not be a problem. (green curve)

In another scenario the pod gets accelerated very smoothly at constant 1,5m/s2 or 456N thrust for 28 seconds and then reduced it to 0.08 m/s2 or 25N thrust for the rest of the time. With this scenario the lowest currents are flowing in the system. The reward from that is a maximum speed of 150 km/h after 1100 meter without overheating any component. (purple curve)

In a last scenario the information from Fig. 2.14a about the efficiencies of different speeds was used to create the most efficient load profile. Therefore up to a speed of 7km/h, 2000N were provided by the motor. Then up to 100km/h it is accelerating for another 6 seconds with 1000N thrust. At the end, up to 162 km/h, 500N thrust were hold before the braking sequence starts. With that load profile the pod reaches 162 km/h after 420 meter without overheating any component. This load profile seems to fit best for the SpaceX Competition and is recommended by the author. (blue curve)

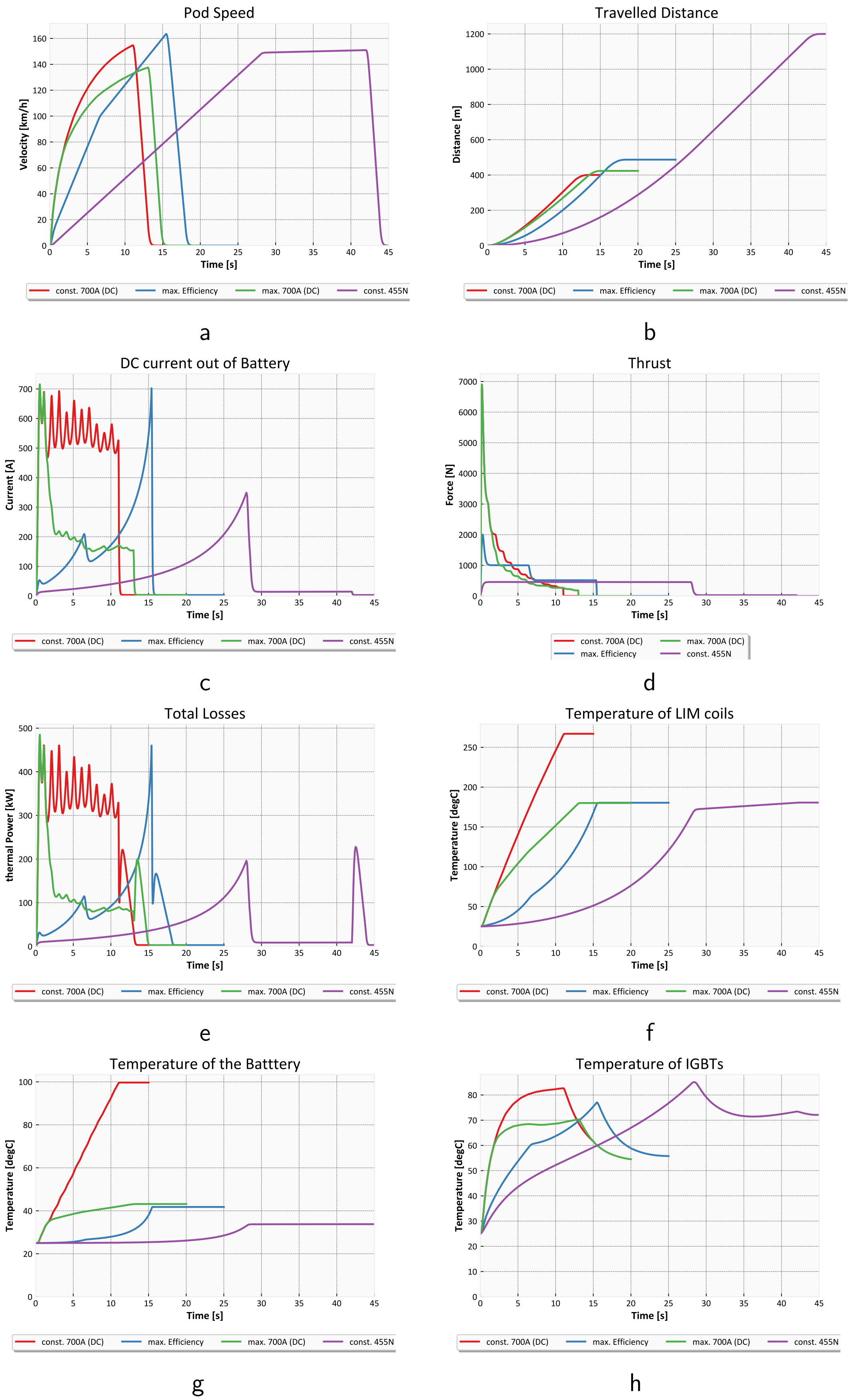

Figure 3.2: Four different load profiles for the SpaceX Competition

3.1.3 Load profile «Eurotube»

The aim of the Eurotube load profile is to quantify the heat sources for a scalable Hyperloop application. The reference system will be the same namely the Swissloop Pod 2019.

In a first scenario the pod will be accelerated with constant 1.5m/s2 up to a velocity of 300km/h. That could be an acceleration for a real future Hyperloop. It is about the acceleration of a «S-Bahn» leaving the station. This scenario will demonstrate what the cooling system will face while accelerated by an onboard short stator LIM. The simulation was made with the ideal Battery model. All more advanced models failed in the simulation because they couldn't provide enough current for the acceleration. We are interested in the thermal power, therefore an infinitely good cooling system shall be applied to keep the temperature of the components at a constant 25°C. A hypothetical future cooling system should be able to handle the same amount of heat as the applied cooling system does to cool the pod successfully.

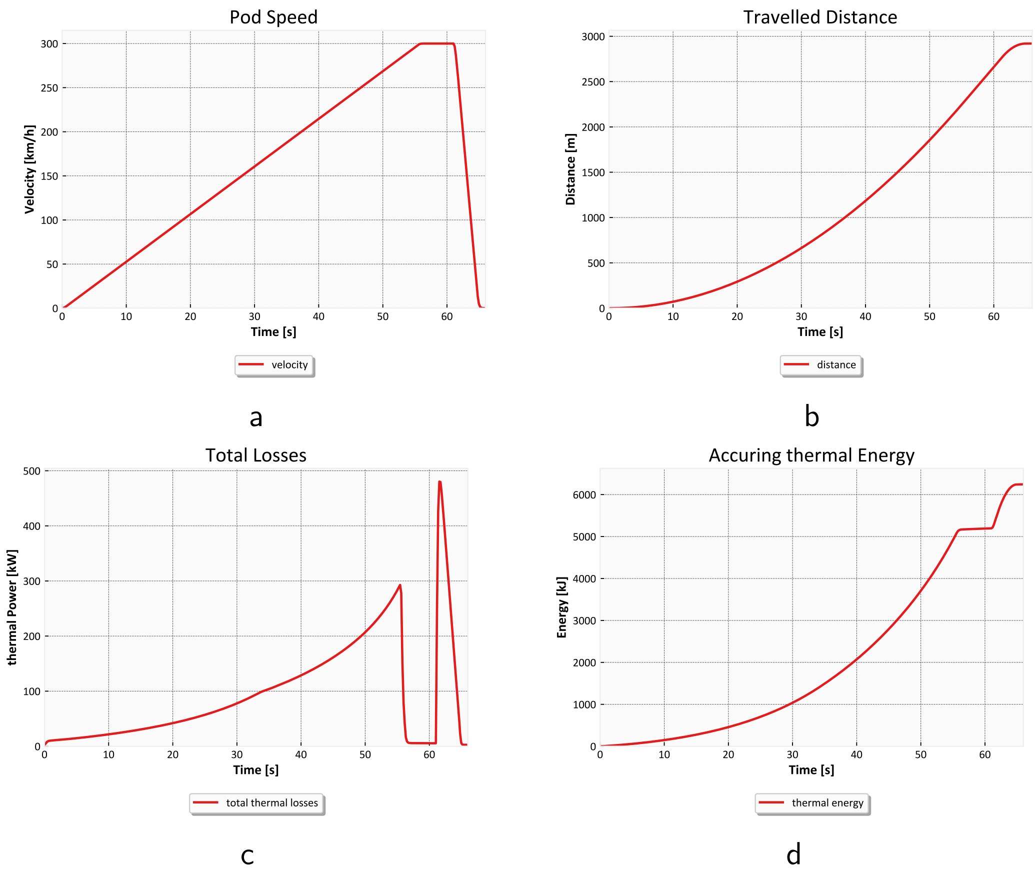

Figure 3.3: Acceleration of the pod with constant 1.5m/s2 to 300km/h on a 3km track

In Fig. 3.3 the results of the simulation are given. Even with constantly 25°C the total amount of thermal losses climbed up to 300kW at 300km/h. While at 100km/h it was as low as 50kW. That shows, what the practice already proved in projects like Transrapid. Short stator linear motors have poor efficiency at high speeds.

Hyperloop alpha already mentioned to mount the linear motor for the acceleration process on the track at the station exits. See Chap. 1.1.2. That would allow the usage of a much longer motor with thicker cross sectional coils and a stationary cooling system not bounded to the low pressure environment inside the tube. On the pod there would be just a small LIM to overcome the drive resistance and to keep the velocity constant. To cover that idea another scenario was simulated. Now an external motor is accelerating the pod to 500km/h. And for 11 seconds the onboard LIM has to hold the speed till the end of the Alphatube. The results on Fig. 3.4c and d show us the amount of power and energy which a cooling system would need to dissipate. The 14kW from the results of 500km/h will rise to 140kW if the pod speed would be 1200km/h. Therefore just to overcome the air drag at the targeted Hyperloop speed of 1200km/h a high power cooling system is needed if the work is done with an onboard LIM.

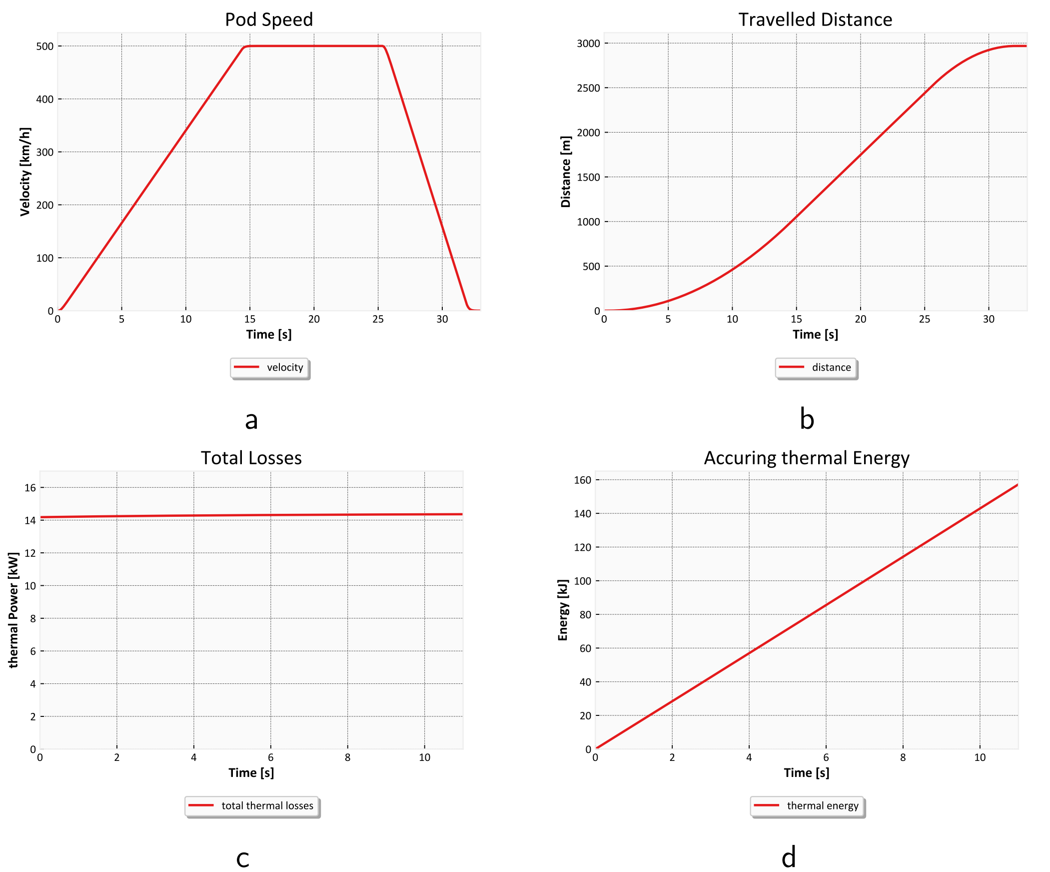

Figure 3.4: Acceleration of the pod with constant 1g from a motor on the track to 500km/h and maintained by the onboard LIM

3.2 Heat absorption

A way must be found to take the heat out of the critical components (Battery, LIM coils, Inverter modules). All the possibilities can be separated in two categories.

One is the **direct absorption** of the heat by the transportation fluid. It is the more challenging but more powerful option. Because bringing a fluid in direct contact to the source has the risk of damaging some important functionalities. Direct absorption can be done by overflowing the heat source surface and absorbing the heat by forced convection. By doing that, the heat is convected directly into the fluid. For good convective performance the heat transfer coefficient has to be as high as possible. Since the heat transfer coefficient depends on the thermal conductivity, Nusselt and Raynolds ($\alpha = f(Nu, Re, \lambda)$) and Nusselt again on Reynolds and Prandtl ($Nu = f(Re, Pr)$), where Reynolds depends on the characteristic length of the surface and the viscosity and the velocity of the fluid ($Re = f(v, L_{char}, \nu)$), good convection depends on a high energetic flowing fluid with good thermal properties. To be a good fluid λ and Pr has to be high and ν has to be low. By providing a large surface area of the source more power can be transmitted by convection. Another possibility of direct absorption is to spray dust on the surface of the heat source and let the transportation fluid vaporise on the surface. Thus a large amount of heat is absorbed with little fluid used. The fluid is heated up to boiling temperature and afterwards gets vaporized. A good fluid for that needs to have a high specific heat capacity, a high enthalpy of vaporisation and a boiling temperature that is well below the critical temperature of the component to be cooled.

Take heat from the source		
conduction	convection	peltier element
$P = A \cdot \frac{\lambda}{x} \cdot \Delta T$	$P = A \cdot \alpha \cdot \Delta T$	$P = \pi \cdot I$
Bringing the source in contact with a conducting solid material	Absorption of the heat by convection from a hot surface	Pumping the heat away from the heat source
sensible heating up	vaporisation	
$P = \dot{m} \cdot c_p \cdot \Delta T$	$P = \dot{m} \cdot \Delta h_v$	
Heat up fluid on a hot surface by overflowing it	Vaporise fluid (dust) on a hot surface	
A: contact surface λ: thermal conductivity x: thickness $\alpha(Nu, \lambda, Re)$: heat transfer coefficient	$\dot{m}$: mass flow Δh_v: enthalpy of vaporisation c_p: specific heat capacity	π: peltier coefficient I: electric current ΔT: change in temperature

Table 3.3: Absorbing the heat from source and transfer it to a fluid. Some possible mechanism

The other is the **indirect absorption** of the heat. Indirect because the transportation fluid never contacts the surface of the heat source itself but is separated from it by a heat conducting solid material. It is the less powerful choice but it is much easier to build. Just bringing a heat conducting material into contact with the surface of the heat source. This will cause a heat flux from the source surface to the material in contact. Letting the transportation fluid flow through that material the heat can be absorbed by convection or vaporisation as described before. These are the same mechanism to move the heat to the transportation fluid but less powerful because the inner surface of the heat conducting material will be less hot than the heat source surface itself. In order to build an efficient cooler block, the arrangement and the geometry of the cooling channels must be smartly designed. See Fig. 3.5 for a possible design.

A special solution is the **peltier element**. It is helpful to enforce the heat to flow more than by natural conduction. When a voltage is applied, heat flows from one side of the element to the other. See Fig. 3.6. The heat flow is proportional to the applied voltage. The factor of proportionality is called peltier coefficient. In that arrangement, the element works as a heat pump and pushes the heat from one side of the element to the other. While one side of the element becomes hot the other is cooling down. A peltier element as a heat pump could be used to active control the temperature of the component to be cooled by applying the correct voltage. The physical mechanism behind the peltier element is the peltier-seebeck effect.

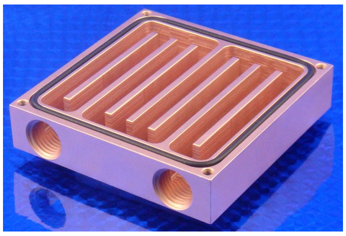

Figure 3.5: Cut through a copper fluid cooler block [13]

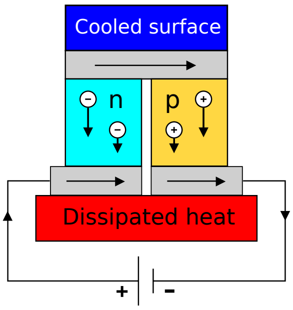

Figure 3.6: Peltier element used as a heat pump for cooling [14]

Battery

The actual installed cooling method used for the Swissloop Pod 2019 Battery is a material that surrounds the cells and serves as a thermal energy storage. This is an isolated cooling method for the Battery packs itself and can not be connected to en external cooling system. This method is not scalable and therefore unsuitable. Two other methods would be to directly flow around the cells with the transportation fluid or installing heat conducting foils between the cells which conduct the heat down or upwards to a fluid cooler block. These three methods are given in Fig. 3.7. The most powerful method is seen to be method (a) by directly flowing around the cells with the transportation fluid.

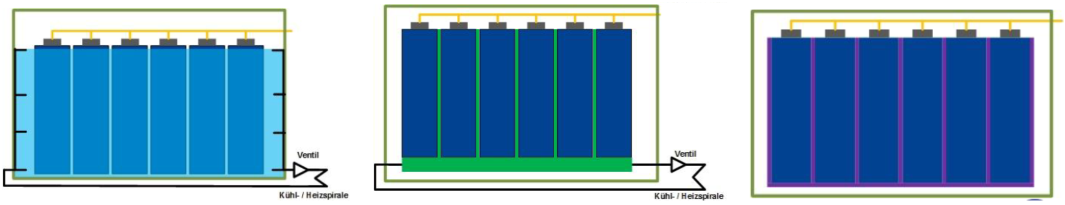

a b c

Figure 3.7: Methods for heat absorption inside a Battery [15]

LIM coils

Only one possibility could be found to take the heat from the LIM coils because the magnetic and electric properties of the motor should not be interrupted by the cooling system. Therefore any direct contact with metals or any other conducting materials must be prevented. Also electrically conductive fluids should not come into contact with the coils. On the outside, the coils are wrapped into a non conductive insulation. This insulation is important for the LIM to work but prevents efficient cooling from the outside. Therefore only cooling from the inside of the copper wires is a potential cooling solution. Allowing an electrical non-conductive liquid to flow through the copper wires is the only way to go. Difficulties are the production of the hollow copper wires for the coils and the choice of a liquid which does not disturb the electrical nor the magnetic functionality of the LIM and offers high thermal properties such as specific heat capacity.

Figure 3.8: Copper hollow conductors to cool the windings of the LIM from the inside [16]

With this method 1 liter thermal oil per second has be heated up by 50°C to take away the 100kW thermal power that is produced by the coils when accelerating the Swissloop Pod 2019 to 200km/h with the LIM.

Inverter modules

The easiest task is to take away the heat from the Inverter modules since they provide a plane surface for cooling. A water cooling block out of copper or aluminium similar to the ones used for cooling CPUs in computers. To be able to control the temperatures of the semiconductor junctions as well as to reach higher cooling performance, a peltier element can be used between the cooling surface of the Inverter modules and the water cooling block. By taking water as the transportation fluid the cooling block would need a flow throughput of 5 liter per minute to heat it up by 30°C if the Inverter modules produces 10kW as observed in Chap. 2.4.

3.3 Heat transport

To transport the heat from the sources to the sink a non compressible liquid fluid has to be taken. Because it can be easily transported using a pump which has a lower energy consumption compared to a compressor for pumping gaseous fluids. It is preferred for many aspects; To pump as little volume flow as possible and to rise the temperature as less as possible during the heat absorption at the sources but still be able to carry away the necessary thermal power.

$$P_{th} = \dot{m} \cdot c_p \cdot \Delta T = \dot{V} \cdot \rho \cdot c_p \cdot \Delta T$$

$$P_{pump} = \dot{V} \cdot \rho \cdot g \cdot H$$

On one hand a fluid with high densities and high specific heat capacity is needed. On the other hand the power consumption of the pump is scaling proportional to the density.And therefore to lower the energy consumption of the pump a low density is needed. In Table 3.4 there are some possible transportation fluids with their relevant properties suited for the application in the Hyperloop cooling system.

	density	specific heat capacity	boiling temperature	enthalpy of vaporisation	thermal conductivity	dynamic viscosity	prandtl number	useful property	source
water	$997.05\,\frac{kg}{m^3}$	$4181.3\,\frac{J}{kg \cdot K}$	$99.97\,°C$	$2256.5\,\frac{kJ}{kg}$	$0.6065\,\frac{W}{m \cdot K}$	$0.89\,mPa \cdot s$	6.136	very high heat capacity	CoolProp
water-glycol (50%-50%)	$1062.2\,\frac{kg}{m^3}$	$3338\,\frac{J}{kg \cdot K}$	$106.1\,°C$	?	$0.3922\,\frac{W}{m \cdot K}$	$3.16\,mPa \cdot s$	26.859	higher boiling temp. than water	CoolProp
thermal oil	$867\,\frac{kg}{m^3}$	$1930\,\frac{J}{kg \cdot K}$	$340\,°C$	-	$0.1276\,\frac{W}{m \cdot K}$	$29.6\,mPa \cdot s$	519.67	electrically non-conductive	Datasheet «Thermoil 55»
ethanol	$785.1\,\frac{kg}{m^3}$	$2434.5\,\frac{J}{kg \cdot K}$	$78.42\,°C$	$849.6\,\frac{kJ}{kg}$	$0.1635\,\frac{W}{m \cdot K}$	$1.08\,mPa \cdot s$	16.116	low boiling temperature	CoolProp

Table 3.4: Properties of different fluids suited for heat transport (at 25°C) [17, 18]

3.4 Heat sink

A heat sink for a Hyperloop system is evaluated, in order to dissipate the collected heat. The standard heat sink of transportation modes is the air cooler. But because of the low pressure environment inside the Hyperloop tube this is not a smart solution.

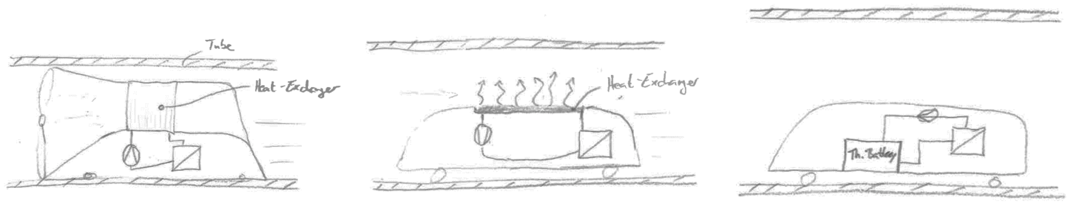

a b c

Figure 3.9: Different heat sinks for Hyperloop pods

3.4.1 Convection

Like many other mode of transport the Hyperloop could be cooled with an air heat exchanger. Installing a finned heat exchanger at the front of the vehicle would let the air stream flow through the heat exchanger. See Fig. 3.9a. With a simple hand calculation it is obvious that the thermal power of this heat sink at 300km/h, collecting all the air available in the tube, would not be enough to cool down the LIM system if it is accelerating the pod. The simulations in Chap. 3.1 were done with an air drag coefficient of 0.12. By pressing all the available air of the tube through a heat exchanger the air resistance will increase enormously. Therefore the produced heat by the system will increase too. That is why this solution is rated to be unsuitable. It would unnecessarily increase the air drag to collect enough air from the low pressure environment.

$$P_{th} = v \cdot A \cdot \rho \cdot c_p \cdot \Delta T \cdot \mu_{he} = 37.6\,kW$$

v	$300\,km/h$	vehicle velocity
A	$0.95\,m^2$	cross-sectional area of the incoming air
ρ	$0.01052\,\frac{kg}{m^3}$	density of air (25°C,900Pa)
c_p	$1004.7\,\frac{J}{kg \cdot K}$	specific heat capacity of air (25°C,900Pa)
ΔT	$50\,°C$	temperature difference (heat exchanger - air)
μ_{he}	0.9	efficiency of the heat exchanger

3.4.2 Radiation

In a partial vacuum environment like the Hyperloop, the idea of emitting the waste heat by radiation seems obvious. By assuming the whole shell of the pod as emitting surface and cover it with a special coating with a high emission factor, the shell would need a temperature of 453°C to emit the same amount of power as the convective heat exchanger does at 300km/h. And that amount of power is even not enough to cool the whole system at full load. Therefore this solution is also rated as unsuitable. To heat up the whole surface of the shell to above 500°C to get a large enough heat sink is ridiculous.

$$P_{th} = \epsilon_1 \cdot \sigma \cdot A_1 \cdot (T_1^4 - T_2^4) = 37.5\,kW$$

solved for T_1: $T_1 = 453°C$

ϵ_1	0.98	emission coefficient
σ	$5.67 \cdot 10^{-8}\,\frac{W}{m^2 \cdot K^4}$	Stefan-Bolzmann constant
A_1	$2.5\,m^2$	emitter surface (whole shell surface)
T_1	?	temperature of the emitter
T_2	$30\,°C$	temperature of the absorber

3.4.3 Thermal energy storage

The last remaining possibility is to store the heat in a thermal capacity on the pod during run and discharge or exchange it at the station.

Sensible TES

There are several thermal energy storage (TES) technologies known. The most widely used technology is the sensible heat storage. There a mass of material is heated up whereby the heat capacity of the material is used to store the energy. To create a small, light storage with a high amount of thermal capacity a material with a low density and high volumetric thermal capacity is needed. In Table 3.5 are different materials listed used for sensible storage systems.

Table 3.6 Thermal capacities at 20 °C of some common TES materials

Material	Density (kg/m^3)	Specific heat (J/kg K)	Volumetric thermal capacity (10^6 J/m^3 K)
Clay	1458	879	1.28
Brick	1800	837	1.51
Sandstone	2200	712	1.57
Wood	700	2390	1.67
Concrete	2000	880	1.76
Glass	2710	837	2.27
Aluminum	2710	896	2.43
Iron	7900	452	3.57
Steel	7840	465	3.68
Gravelly earth	2050	1840	3.77
Magnetite	5177	752	3.89
Water	988	4182	4.17

Table 3.5: Materials properties used for sensible heat storage[19]

But even with water as the best sensible material, 20 liter would be required to store 5MJ of thermal heat. Which is the heat produced in a acceleration of the pod to 300km/h as seen in Chap. 3.1.

$E_{th} = \rho \cdot V \cdot c_p \cdot (T_2 - T_1)$
solved for V:
$V = 0.02\,m^3 \approx 20\,l$

E_{th}	$5\,MJ$	amount of thermal energy
ρ	$997.05\,\frac{kg}{m^3}$	density of water (25°C)
V	?	Volume of the storage
c_p	$4181.3\,\frac{J}{kg \cdot K}$	specific heat capacity of water (25°C)
T_1	$20\,°C$	start temperature of the storage
T_2	$80\,°C$	end temperature of the storage

The thermal power that can be absorbed by the sensible storage depends on the temperature difference between the storage material and the transportation fluid, as well as on the size of the heat exchanger surface in the storage.

Latent TES

Another TES which works very similar to the sensible technology is the latent TES. Here also a mass of material is heated up, but the material is chosen so that during the heating up it changes its phase from solid to liquid. During phase transition, the material can absorb a lot of energy without increasing its temperature. Therefore for the same rise in temperature the material is able to store more energy than in sensible temperature regions. The amount of energy stored in the material related to its temperature is given in Fig. 3.10. The important property for latent energy storage is the enthalpy of fusion (Δh_{pc}). As seen in the below hand calculation, by using the phase change with the same rise in temperature (60°C) just 8.7 liter instead of 20 liter water will be required to store the 5MJ of thermal heat.

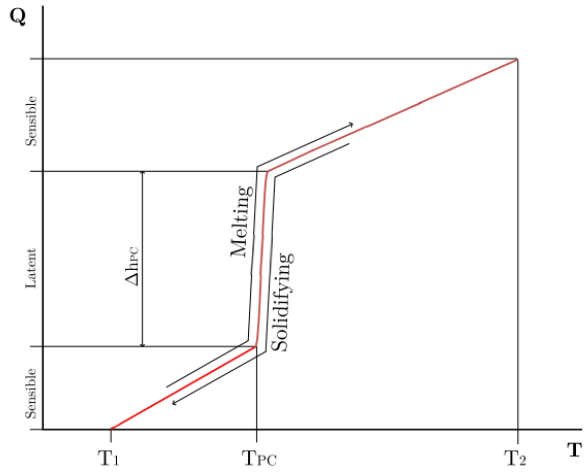

Figure 3.10: Warm up curve of a PCM material from T1 to T2 through its phase change region [20]

The difficulty of latent TES is to find a material that has the phase transition zone from solid to liquid at a temperature that is within the working range of the application. In our case the cooling system would work somewhere between the temperature of the regeneration liquid and well below the critical temperature of the components.

$$E_{th} = \rho \cdot V \cdot (h_{s,s} + \Delta h_{pc} + h_{s,l})$$
$$h_{s,s} = c_{p,s} \cdot (T_m - T_1)$$
$$h_{s,l} = c_{p,l} \cdot (T_2 - T_m)$$
solved for V:
$$V = 0.0087\, m^3 \approx 8.7\, l$$

E_{th}	$5\, MJ$	amount of thermal energy
ρ	$997.05\, \frac{kg}{m^3}$	density of water (25°C)
V	?	Volume of the storage
$c_{p,s}$	$2220\, \frac{J}{kg \cdot K}$	specific heat capacity of solid water (-10°C)
$c_{p,l}$	$4181.3\, \frac{J}{kg \cdot K}$	specific heat capacity of liquid water (25°C)
Δh_{pc}	$333.55\, \frac{kJ}{kg}$	enthalpy of fusion of water
T_m	$0\,°C$	melting temperature of the PCM
T_1	$-5\,°C$	start temperature of the storage
T_2	$55\,°C$	end temperature of the storage

Like in sensible storage, the power that can be absorbed by the latent storage depends on the temperature difference between the storage material and the transportation fluid, as well as on the size of the heat exchanger surface in the storage. The problem in latent TES will be to build a heat exchanger inside the tank that gives the application enough thermal power.

Thermochemical TES

In thermochemical TES a material or fluid composed of two components is used to store the energy. The two components together build a material which has a lower energy potential than the two components as individual materials. When charging the thermochemical TES the material composed of the two components is cracked into two individual materials containing one component each. The cracking absorbs thermal energy and therefore this process can be seen as charging the TES. When bringing the two materials together again and letting them combine to the one material containing both components, energy is released in form of heat. The TES is discharging.

Thermochemical TES distinguishes between Sorption and reversible chemical Reactions.

Sorption is a physical or chemical process through which a substance (sorptive) becomes attached to the surface or volume of a solid or liquid substance (sorbent). The process of attaching sorptive to the sorbent is called adsorption and its releasing thermal energy. The charging process is called desorption and corresponds to sorbtive leaving the sorbent. In that process thermal energy is consumed. In applications the sorptive is transported through a bulk of sorbent by a transportation fluid. In most cases the transportation fluid is air because it flows easily through the bulk without too much pressure drop. This makes the charging and discharging of a sorptive TES a complex process and accordingly requires expensive and large systems. Even this technology would offer very high energy densities it is considered as unsuitable for a compact application in vehicles.

Reversible chemical reactions are chemical processes, which can be reversed as often as desired and run accordingly exothermically or endothermically. Charging is the endothermic and dissotiative direction of the chemical reaction. To separate the two species, the energy amount of the enthalpy of formation or the heat of reaction is consumend. To discharge the TES the two separated species are brought together. In the following recombining and exothermal reaction the stored heat will be released. The materials suitable for reversible chemical reaction TES are difficult to handle. They need to have special pre-processing systems to bring them in the right conditions for the reaction. Additionally there is the fact that this technology is still under heavy research and almost no suppliers can be found on the market. Therefore this technology is considered as unsuitable at the moment even it offers the highest energy densities and the possibility of very high thermal power , if the chemical kinetics of the reaction is fast enough.[20]

3.5 Cooling system

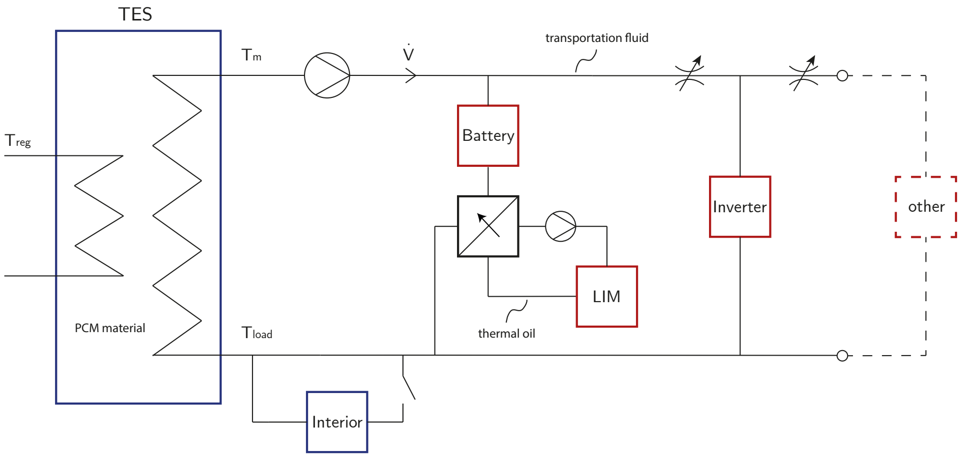

Figure 3.11: Schematic of the recommended onboard cooling system for Hyperloops. Red: heat sources, blue: heat sinks

The recommended cooling system is given in Fig. 3.11. It is based on a TES tank filled with a PCM material. Depending on the selected PCM material, the temperature potentials (T_m and T_{load}) will be different in the system. The heat sources «Battery» and «LIM» are connected in series because the Battery should be kept below 45°C and therefore the heated fluid from the Battery still has a maximum temperature still cool enough to cool the LIM. In addition, the cooling requirements of the Battery and the LIM increase at the same rate and in series they will be flowed through with the same volume flow rate. The LIM needs thermal oil for cooling where the transportation fluid is water. That is why it has a separated circulation with a heat exchanger to give away the heat from the LIM circle to the transportation fluid. The Inverter as well as the other small heat sources are connected to the cooling circuit in parallel to the Battery and LIM. The Interior (cabin with the passengers) can be connected as an additional heat sink in front of the storage tank if it needs to be heated.

The most critical design parameter of the cooling system will be the thermal power that needs to be dissipated from the sources. To have a powerful cooling system, the volume flow ($\dot{V}$) of transportation fluid has to be high enough and the heat exchanger in the storage tank has to be big enough in order to transfer the thermal power to the PCM. The driving force to exchange heat from the transportation fluid to the PCM is the temperature difference between them. In Fig. 3.12a a qualitative temperature profile of the PCM during charging is given. The temperature difference is in a large range dependent on the melting temperature (T_m) of the PCM. Therefore the PCM material must be selected so that T_m is as low as possible. If a PCM with a high λ_l is chosen, the PCM will conduct the heat better and therefore the melting process will be better. This results in a higher absorption of thermal power. By inspecting Table 3.6, water is the best PCM material resulting in a TES application with most thermal power.

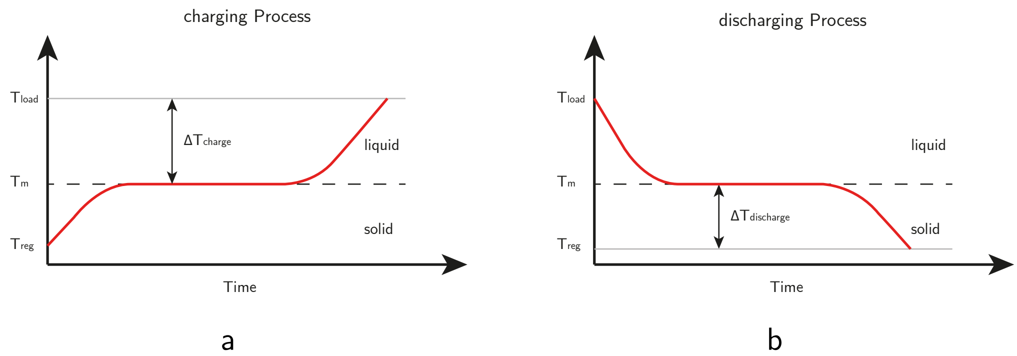

Figure 3.12: temperatures of the charging (a) and discharging (b) process of a latent TES system

On the other hand the discharging power of the system defines the waiting time of the Hyperloop at the station. The bigger the heat exchanger for discharging and the larger $\Delta T_{discharge}$ the faster the storage can be regenerated and the sooner the Hyperloop can leave the station again. From this point of view water is not the best PCM any more. A PCM with a high melting temperature will perform better while discharging. But still heat conductivity (λ_l) has to be high in order to crystallise fast. Therefore salcium chloride hexahydrate would be best for fast and easy discharging. Because of its crystallisation temperature of 30°C, cool water could be used for the regeneration while for water as PCM a fluid well below 0°C needs to be processed for discharging.

	formula	type	T_m	Δh_{pc}	ρ_s	λ_l	$c_{p,l}$	$c_{p,s}$
Water	H_2O	-	$0\,°C$	$333.55\,\frac{kJ}{kg}$	$916.8\,\frac{kg}{m^3}$	$0.597\,\frac{W}{m\cdot K}$	$4181.3\,\frac{J}{kg\cdot K}$	$2220\,\frac{J}{kg\cdot K}$
Calcium chloride hexahydrate	$CaCl_2 \cdot 6H_2O$	salt hydrate	$30\,°C$	$180\,\frac{kJ}{kg}$	$1802\,\frac{kg}{m^3}$	$0.54\,\frac{W}{m\cdot K}$	$1562\,\frac{J}{kg\cdot K}$	$1802\,\frac{J}{kg\cdot K}$
Decosane	$C_{22}H_{46}$	paraffin	$44\,°C$	$250\,\frac{kJ}{kg}$	$791\,\frac{kg}{m^3}$	$0.15\,\frac{W}{m\cdot K}$	$2380\,\frac{J}{kg\cdot K}$	$1930\,\frac{J}{kg\cdot K}$
1-Hexadecanol	$C_{16}H_{34}O$	alcohol	$49\,°C$	$235\,\frac{kJ}{kg}$	$973\,\frac{kg}{m^3}$	$\sim 0.15\,\frac{W}{m\cdot K}$	$2550\,\frac{J}{kg\cdot K}$	$1740\,\frac{J}{kg\cdot K}$

Table 3.6: Properties of different possible PCM [21]

With Table 3.7 it is possible to get an idea of how big and how heavy the tank for the chosen PCM in the cooling system will become. The data in Table 3.7 are based on a PCM tank share of 50%. That means 50% of the tank is filled with PCM the rest of the space is taken by the heat exchangers for charging and discharging. With the properties of the PCM and the ones for the transportation fluid, some specific values for capacity and price can be calculated for each of these PCM materials.

PCM material	PCM tank share	heat transportation fluid	temperatures (T_{reg}, T_{load})	volume specific capacity	mass specific capacity	capacity specific price
Water	50%	water-glycol	$-5\,°C, 80\,°C$	$394.7\,\frac{MJ}{m^3}$	$0.412\,\frac{MJ}{kg}$	$80.0\,\frac{CHF}{MJ}$
Calcium chloride hexahydrate		water	$25\,°C, 80\,°C$	$365.7\,\frac{MJ}{m^3}$	$0.261\,\frac{MJ}{kg}$	$87.5\,\frac{CHF}{MJ}$
Decosane				$259.5\,\frac{MJ}{m^3}$	$0.290\,\frac{MJ}{kg}$	$84.5\,\frac{CHF}{MJ}$
1-Hexadecanol				$285.6\,\frac{MJ}{m^3}$	$0.290\,\frac{MJ}{kg}$	$85.0\,\frac{CHF}{MJ}$

Table 3.7: Specific capacity and price of the different PCM for a 5MJ system

In Table 3.8 there is an overview of the pros and cons of the two favorite PCMs.

Water	**Calcium chloride hexahydrate**
+ high thermal capacity and charging power + little and low priced PCM material	+ high thermal power when discharging + regeneration at the stations with cold water
- water-glycol as transportation fluid (low c_p-> more volume flow -> more pumping power) - complex and expensive refrigeration system at the stations	- less thermal capacity and charging power - more expensive storage

Table 3.8: Pros and cons of Water and Calcium chloride hexahydrate as PCM

3.5.1 Specifications of the cooling system

The calcium chloride hexahydrate as PCM is chosen. Because it allows to use water as transportation fluid. Which has the better properties as the water-glycol. Therefore less transportation fluid needs to be circulated in the cooling circuit. This allows to save money, weight and energy consumption of the cooling circuit because a smaller pump and smaller pipe diameters can be chosen. Additionally the discharging process at the stations are much simpler because cold water can be used. The money for all the expensive refrigeration systems at the stations which would be needed for water as PCM, can be saved too.

With calcium chloride hexahydrate as PCM the tank for 5MJ capacity will be $0.0137\, m^3$ and 19.15kg. It is assumed to double the weight of the tank for having the weight for the whole cooling system including heat exchangers, piping, pumps and the TES. This will result in about 40kg for the cooling system, which is sufficient for 200km/h with LIM acceleration or maintaining a speed of 1200km/h with the LIM.

Chapter 4

Conclusion

Thanks to the system model of the representative Pod «Claude Nicollier», the system behavior could be analysed. It has been observed that the two most relevant loss mechanisms are the end effects due to the LIM length and the joule heating due to resistive losses in the electrical components. While the end effects scale with the pod speed only, the joule heating increases with both the speed as well as the material temperature. That is because it scales with the current in square and the current itself scales because of the end effects. Additionally the joule effect creates heat which increases the temperature of the resistive material and therefore affects itself negatively. The temperature increase due to joule heating is a vicious circle and must be prevented by effective cooling. But also the Inverter losses are not small. Because of the constantly high switching frequency, the Inverter produces a heat base-load which also increases slightly with temperature.

It was possible to establish a correlation between the size of the current density in the LIM windings and the heat production relevance of the components. Up to a current density of $15\,\frac{A}{mm^2}$ the Inverter losses are dominant. This is mostly the case for very low speeds. In the range between $15\,\frac{A}{mm^2}$ and $25\,\frac{A}{mm^2}$ the heat production in the LIM coils are dominant. That correspond to most of the operating points of the pod up to very high speeds. Therefore the joule heating in the LIM is over a large range of operating points the most relevant heat producing component. All above a current density of $25\,\frac{A}{mm^2}$ the Battery becomes the problematic component. Because at such high currents in the LIM, the total heat production becomes enormous and therefore the discharging current of the Battery explodes. Ones reaching that point, no cooling system will be able to manage the heating power of the system anymore.

With an efficiency analysis, the best point of the powertrain could be determined. It could be shown that the uncooled reference system has its best-point of 19.4% total efficiency at a speed of 50km/h and a thrust force of the LIM of 750N. The best efficiency at low speeds is achieved with maximum thrust, while at high speeds small thrusts are more efficient. With a powerful cooling system the systems overall best-point could be raised to 21%. Low thrusts profits more from a cooling system than high thrusts.

With the knowledge of the system efficiencies an optimal load profile was determined for the Swissloop team to reach highest possible speeds at the SpaceX Hyperloop Pod Competition. By running the system at all times close the the best efficiency point it would be possible to reach 160km/h with «Claude Nicollier» at the competition.

In order to obtain the capacity and performance specifications for the cooling concept, the system model was simulated and evaluated with two different load profiles. On one hand, the onboard LIM accelerates constantly at 1.5m/s2 to a speed of 300km/h. This acceleration corresponds to a «S-Bahn» leaving the station. The thermal power output increases to 300kW and a total thermal energy of 5MJ is generated during acceleration. On the other hand, an external linear motor mounted on the track will take over the acceleration of the pod. While the onboard LIM has to maintain the speed during run. Unlike before, the pod is accelerated with 1g to 500km/h. To maintain the 500km/h a thermal power output of 14kW and a total thermal energy of 0.2MJ is generated on the 3km Alphatube test track. If the speed was 1200km/h, 140kW thermal power would be generated to overcome the air drag. This corresponds to the intended Hyperloop speed.

This numbers are used to design a possible cooling system for a future Hyperloop pod. Different possibilities for absorbing the heat at the sources were compared. For each component the best solution to absorb the heat was evaluated. So the cells in the Battery packs will directly be flushed with transportation fluid. The LIM windings will be flowed through from the inside of the conductors with a suitable thermal oil. And the Inverter modules will be fitted with a fluid cooler block and a peltier element in between for controlling the temperature of the semiconductors. The heat sink of the system will be a thermal energy storage tank which will be charged during run and discharged at the stations. The best suited technology at this time is latent TES. As PCM, calcium chloride hexahydrate is chosen because of its practical melting temperature of 30°C. This melting temperature allows an easy regeneration with cold water at the stations and the possible usage of water as transportation fluid in the cooling circuit. With this concept a high power TES tank with a thermal capacity of 5MJ has a dimension of $0.014\,m^3$ in space and 19kg in mass. Additional space and mass will be needed for the heat exchangers, the piping and the pumps.

Chapter 5

5 Outlook

This work shows a high level design for a future Hyperloop cooling concept. And it also shows, that an efficient cooling system is an important part of a Hyperloop system which drives longer than just a few seconds. To be able to really build a pod with such a cooling system onboard, a lot of detailed questions still have to be clarified and more will appear during realisation. For example the designing of the heat exchangers, the evaluation of the volume flows or the design of the storage tank to be able to crystallise and melt the PCM with high performance.

The powertain of the pod itself also has a great potential for improvements in terms of heat production. The problem of joule heating could be reduced by a higher system voltage or larger wire cross-sections. It could be considered to build a long stator linear motor in the track for acceleration and using the LIM as an onboard motor to overcome the air resistance between the stations. Apparently synchronous linear motors work more efficient than the asynchronous ones like the LIM. Changing the technology could also reduce the heat generation.

This work shows that there are still many topics to work on before a Hyperloop could become reality...

Bibliography

[1] UNO, Mamoru: Chuo Shinkansen Project using Superconducting Maglev System. In: *Japan Railway & Transport Review* (2016), Oktober, Nr. 68, S. 14–25

[2] KEMPLER, Hermann: Die "Rohrbahn". In: *Berliner Illustrirte Zeitung* (1938), August, Nr. 33

[3] KEMPLER, Hermann: *Schwebebahn mit raederlosen Fahrzeugen, die an eisernen Fahrschienen mittels magnetischer Felder schwebend entlang gefuehrt werden*. 1937

[4] BESLER, Ilyas: *Energy Analysis of a Hyperloop System in Europe*, ETHzürich, Diplomarbeit, 2018

[5] TRANCOSSI, Michele: What price of speed? A critical revision through constructal optimization of transport modes. In: *International Journal of Energy and Environmental Engineering* (2015), Februar

[6] MUSK, Elon: Hyperloop Alpha / SpaceX. 2013. – Forschungsbericht

[7] LUCERNE, World Tourism F.: Start-Up Winner Category Mobility: Eurotube, 2019

[8] TIMPERIO, Christopher L.: *Linear Induction Motor (LIM) for Hyperloop Pod Prototypes*, ETHzürich, Diplomarbeit, 2018

[9] SWISSLOOP: Final Design Package / Swissloop. 2019. – Forschungsbericht

[10] MODELICA (Hrsg.): *Modelica Standard Library documentation*. Modelica, 2017. https://doc.modelica.org/

[11] Eisenverluste. In: *ACADEMIC* (2005). https://deacademic.com/dic.nsf/dewiki/381399

[12] LAVINE, Frank P. Incropera; David P. Dewitt; Theodore L. Bergman; Adrienne S.: *Fundamentals of Heat and Mass Transfer*. John Wiley & Sons, 2007. – ISBN 978–0–471–45728–2

[13] WBA-3.0-0.85-CU-01 Water Block. In: *Custom Thermoelectric* (2019). https://customthermoelectric.com/water-block-3-0-x-3-0-x-0-85-copper.html

[14] Wikipedia: *Thermoelectric effect*. https://en.wikipedia.org/wiki/Thermoelectric_effect. Version: 2019

[15] Becher, Daniel: *Silicone als Sicherheits-und Elastomer-elemente in Lithium-Ionen Batterien*. 2018

[16] Luvata: *Copper hollow conductors*, 2018

[17] Solutia: *Therminol 55*. Solutia Inc., 2008

[18] CoolProp Team (Hrsg.): *CoolProp Documentation*. CoolProp Team, 2019. http://www.coolprop.org/coolprop/index.html

[19] Rosen, Ibrahim Dincer; Marc A.: *Thermal energy storage. systems and applications*. Wiley, 2011

[20] Worlitschek, Lorentz Gubler; Vinzenz Härri; Anastasia Stamatiou; J.: Energy Storage Systems. (2017)

[21] Stephan, Prof. Dr.-Ing. P.: *VDI-Wärmeatlas*. Springer, 2013. – ISBN 978–3–642–19982–0

[22] Schenk, Marcus Debald; Damaris Nehrdich; F.: Transrapid - revolutionäre Fortbewegungstechnologie eines neuen Zeitalters und seine gegenwärtigen Durchsetzungsschwierigkeiten in Deutschland. 2002. – Forschungsbericht

[23] Carrel, Ulrich Weidmann; Stefan Buchmüller; Markus Rieder; Alexander Erath; Andrew Nash; A.: Europäische Marktstudie für das System Swissmetro Phase I / ETHzürich. 2006. – Forschungsbericht

[24] J.Fleig, M.Einhorn; F.V.Conte; C.Kral; C.Niklas; H.: A Modelica Library for Simulation of Elecric Energy Storages / AIT Austrian Institute of Technology. 2011. – Forschungsbericht